QUANTITATIVE EVALUATION OF THE "SELF-DEVELOPMENT" PROCESS IN EXTRATROPICAL CYCLOGENESIS

Cecil Jackson Folker

THESIS

QUANTITATIVE EVALUATION OF THE
"SELF-DEVELOPMENT" PROCESS
IN EXTRATROPICAL CYCLOGENESIS

by

Cecil Jackson Folker

March 1975

Thesis Advisor: M.S. Tracton

REPORT DOCUMENTATION PAGE

READ INSTRUCTIONS BEFORE COMPLETING FORM

1. REPORT NUMBER

2. GOVT ACCESSION NO.

3. RECIPIENT'S CATALOG NUMBER

4. TITLE (and Subtitle)
Quantitative Evaluation of the "Self-Development" Process in Extratropical Cyclogenesis

5. TYPE OF REPORT & PERIOD COVERED
Master's Thesis; March 1975

6. PERFORMING ORG. REPORT NUMBER

7. AUTHOR(s)
Cecil Jackson Folker

8. CONTRACT OR GRANT NUMBER(s)

9. PERFORMING ORGANIZATION NAME AND ADDRESS
Naval Postgraduate School
Monterey, California 93940

10. PROGRAM ELEMENT, PROJECT, TASK AREA & WORK UNIT NUMBERS

11. CONTROLLING OFFICE NAME AND ADDRESS
Naval Postgraduate School
Monterey, California 93940

12. REPORT DATE
March 1975

13. NUMBER OF PAGES
69

14. MONITORING AGENCY NAME & ADDRESS(if different from Controlling Office)

15. SECURITY CLASS. (of this report)
Unclassified

15a. DECLASSIFICATION/DOWNGRADING SCHEDULE

16. DISTRIBUTION STATEMENT (of this Report)
Approved for public release; distribution unlimited.

17. DISTRIBUTION STATEMENT (of the abstract entered in Block 20, if different from Report)

18. SUPPLEMENTARY NOTES

19. KEY WORDS (Continue on reverse side if necessary and identify by block number)
Extratropical Cyclogenesis

20. ABSTRACT (Continue on reverse side if necessary and identify by block number)

The objective of this study is to assess quantitatively the process of "self-development" (Sutcliffe and Forsdyke, 1950) in extratropical cyclogenesis. The basic approach is to determine within the framework of the quasi-geostrophic equations the contributions of thermal advection and latent heat release to changes occurring in the intensification rate of a surface cyclone which result from modifying the field of

(20. ABSTRACT Continued)

vorticity advection. The relevant concepts and equations are applied to a major cyclone over the central United States and to a structurally simple analytic model of a cyclonic disturbance for which varying horizontal and vertical distributions of latent heat release are prescribed.

Results of computations utilizing the analytic model indicate that the effect of latent heat release in self-development can be comparable with that of thermal advection. The separate and, more so, the collective influence of these mechanisms upon acceleration of the deepening rate are considered synoptically significant; however, the influence of translation of the vorticity maximum aloft with respect to the surface system appears to dominate changes in the rate of development. The quantitative reliability of the results obtained for the real data case are in doubt because of apparent difficulties in the objective scheme (HOBAN) employed in analysis of input data.

Quantitative Evaluation of the "Self-Development" Process in Extratropical Cyclogenesis

by

Cecil Jackson Folker
Lieutenant, United States Navy
B.S., Auburn University, 1967

Submitted in partial fulfillment of the
requirements for the degree of

MASTER OF SCIENCE IN METEOROLOGY

from the

NAVAL POSTGRADUATE SCHOOL
March 1975

ABSTRACT

The objective of this study is to assess quantitatively the process of "self-development" (Sutcliffe and Forsdyke, 1950) in extratropical cyclogenesis. The basic approach is to determine within the framework of the quasi-geostrophic equations the contributions of thermal advection and latent heat release to changes occurring in the intensification rate of a surface cyclone which result from modifying the field of vorticity advection. The relevant concepts and equations are applied to a major cyclone over the central United States and to a structurally simple analytic model of a cyclonic disturbance for which varying horizontal and vertical distributions of latent heat release are prescribed.

Results of computations utilizing the analytic model indicate that the effect of latent heat release in self-development can be comparable with that of thermal advection. The separate and, more so, the collective influence of these mechanisms upon acceleration of the deepening rate are considered synoptically significant; however, the influence of translation of the vorticity maximum aloft with respect to the surface system appears to dominate changes in the rate of development. The quantitative reliability of the results obtained for the real data case are in doubt because of apparent difficulties in the objective scheme (HOBAN) employed in analysis of input data.

TABLE OF CONTENTS

LIST OF TABLES

LIST OF FIGURES

ACKNOWLEDGEMENTS

The author gratefully acknowledges Professor M.S. Tracton, the author's thesis advisor, for his advice and encouragement. Only through his patience and understanding was this study completed.

Finally, special acknowledgement is extended to the author's wife, Sue, and family, Tim and Angel, for their understanding the long hours spent in research and preparation of this thesis.

I. INTRODUCTION

A. OBJECTIVE

Significant weather in middle-latitudes is almost invariably associated with the development of extratropical cyclones. Not surprisingly, therefore, the physical and dynamical mechanisms responsible for cyclogenesis have been subjects of considerable inquiry. The object of such inquiry has been to understand more fully the workings of extratropical cyclones, formulate their governing laws, and accurately predict or even control the associated weather. Since there are several excellent sources[1] which summarize and synthesize existing concepts of cyclogenesis in middle-latitudes, no attempt will be made here to review the subject.

This thesis concerns the particular aspect of extratropical cyclogenesis referred to by Sutcliffe and Forsdyke (1950) as "self-development." Specifically, the objective of this investigation is to assess quantitatively the importance of the self-development process and determine the relative influence of the contributing mechanisms. Although, qualitatively, self-development is readily comprehensible and seemingly important, quantitative assessment of this process, to the best knowledge of this investigator, has not been documented in the literature.

---

[1]Of particular note are the books of Petterssen (1956), Palmen and Newton (1969), and the thesis of Downey (1972).

B. SELF-DEVELOPMENT

As discussed by Palmen and Newton (1969), self-development is the process wherein progressive deformation of the upper current in the vicinity of a cyclone, as affected by changes in the thermal structure of the troposphere, results in a progressive increase of the upper-level vorticity advection and consequent intensified development of the surface low. The process is schematically illustrated in Fig. 1. Subsequent to the initiation of cyclogenesis, as the cyclone achieves a significant circulation, warm advection ahead and cold advection behind the developing low center deforms the thermal field in the manner shown by Fig. 1. Deformation of the mean isotherms (i.e., thickness lines) through the layer considered can be identified hydrostatically with the growing amplitude of the upper-level contour pattern. The increasing amplitude of the upper wave corresponds to an enhanced variation of the vorticity (as expressed by the curvature) and, therefore, to an increase of the vorticity advection along the upper current over the surface low. This, in turn, implies an increase in the upper-level divergence, which favors progressively stronger low-level convergence and intensification of the cyclone. Note that at each instant of time thermal advection primarily contributes directly only to motion, rather than to development of the sea-level (or 1000 mb) system. That is, at a given instant, the pattern of thermal advection acts primarily to create low-level cyclonic vorticity ahead of the low and anticyclonic

vorticity behind it, thereby accelerating the low along a path directed from the region of maximum cold to maximum warm advection. At that same time, though, the thermal advection tends to enhance the primary deepening mechanism,[2] namely the vorticity advection over the surface low.

If only horizontal temperature advection were important in producing thermal changes in the troposphere, an unbounded deformation of the thermal field and upper flow would be implied. Unbounded increases in amplitude of the upper wave does not occur, however, because adiabatic cooling and warming associated with vertical motions dampen the influence of thermal changes associated with temperature advection. In other words, cooling accompanying ascent and warming accompanying descent in the regions of warm and cold advection, respectively, tend to counteract the influence of horizontal thermal advection. Since the magnitude of vertical motions increase as the developing circulation intensifies, the influence of thermal advection is eventually balanced by the opposing influence of vertical motion. Thus, the process of self-development calls into play a "self-limiting" process that prevents development from proceeding without bound.

In addition to the influence of thermal advection and vertical motion, thermal changes in the troposphere can be produced by condensational heating. Precipitation and the

---

[2]Discussion here is exclusive of the direct influence of latent heat release.

concomitant release of latent heat as, for example, might occur ahead of the surface low center and in advance of the warm front would result in greater amplification of the upper ridge downstream from the low than would be the case if warm advection and adiabatic cooling were the only processes operative. Self-development would then proceed further and the cyclone achieve greater intensity than if precipitation were absent.

C. BASIC APPROACH

As noted, the goal of this investigation is to quantitatively assess the process of self-development. The basic approach is to determine, within the framework of the quasi-geostrophic equations, the magnitude and relative influence of the contributing mechanisms. More specifically, determination is made of the contributions of thermal advection and latent heat release to changes occurring in the intensification (i.e., deepening) rate of a surface cyclone which result from modifying the field of vorticity advection.[3] The relevant concepts and computations are applied to a structurally simple analytic model of cyclonic and anticyclonic disturbances in the baroclinic westerlies (after Sanders, 1971) and to a major cyclone over the central United States, 1200 GMT 10 December 1971.

---

[3]The effect of vertical motions within the quasi-geostrophic framework appears implicitly in tempering the influence of thermal advection and latent heat release, rather than explicitly as a separate contributing mechanism.

II. FORMULATION OF THE PROBLEM

A. QUASI-GEOSTROPHIC FRAMEWORK

It is assumed that atmospheric flow is governed by the quasi-geostrophic vorticity equation

$$\frac{\partial \zeta}{\partial t} = -V\cdot\nabla(\zeta+f) + f_o \frac{\partial \omega}{\partial p} \tag{1}$$

and by the thermodynamic equation

$$\frac{\partial}{\partial t}\left(\frac{\partial \phi}{\partial t}\right) = -V\cdot\nabla \frac{\partial \phi}{\partial p} - \sigma(p)\omega - \frac{R}{C_p p} H \ , \tag{2}$$

where ζ is the relative vorticity; ω is the vertical velocity, $\frac{dp}{dt}$; f_o is a constant value of the coriolis parameter; $\frac{\partial \phi}{\partial t}$ is the geopotential tendency; R is the gas consant for dry air; C_p is the specific heat for dry air at constant pressure; $H = \frac{dQ}{dt}$ is the diabatic heating; and $\vec{V} = \frac{1}{f_o} \vec{k} \times \nabla\phi$ is the geostrophic wind.

When the geostrophic relationship, $\zeta = \frac{1}{f_o} \nabla^2\phi$, is used to express the vorticity, (1) becomes

$$\nabla^2 \frac{\partial \phi}{\partial t} = -f_o V\cdot\nabla(\zeta+f) + f_o{}^2 \frac{\partial \omega}{\partial p} \ . \tag{3}$$

Combination of (2) and (3) in order to eliminate $\frac{\partial \phi}{\partial t}$ yields the quasi-geostrophic omega equation (see, e.g., Holton, 1973),

$$(\sigma\nabla^2 + f_o^2 \frac{\partial^2}{\partial p^2})\omega = f_o \frac{\partial}{\partial p} [V\cdot\nabla(\frac{1}{f_o} \nabla^2\phi + f)] \quad (1)$$

$$- \nabla^2(V\cdot\nabla \frac{\partial\phi}{\partial p}) \quad (2)$$

$$- \frac{R}{C_p} \frac{1}{p} \nabla^2 H \quad . \quad (3)$$

$$(4)$$

The solution of this equation yields values of ω and, hence, $\frac{\partial\omega}{\partial p}$ which enable solution of (3) for the field of geopotential tendency.

The quasi-geostrophic equations in the above or related forms have been utilized widely (e.g., Sanders, 1971; Stuart, 1971; Danard, 1964) in determination of fields of vertical motion and/or geopotential tendency associated with the forcing functions on the right-hand side of (4): differential vorticity advection, term 1, Laplacian of thermal advection, term 2, and Laplacian of diabatic heating, term 3. In this investigation emphasis is not to determine the direct influence of the forcing processes upon the fields of vertical motion or surface geopotential, but rather to evaluate their effect upon self-development. That is, attention is focused upon the influence of the respective mechanisms upon the field of vorticity advection and the resultant changes that would be expected in the intensification rate of a surface cyclone.

Application of (1) to a level near the ground at the center of a cyclone (i.e., at the vorticity maximum where

$\nabla(\zeta+f) \tilde{=} 0$) yields the following expression for surface development in terms of the rate of vorticity production by low-level convergence:

$$\frac{\delta \zeta}{\delta t} = f_o \frac{\partial \omega}{\partial p} \quad . \tag{5}$$

Equivalently, one can write

$$\nabla^2 \frac{\delta \phi}{\delta t} = f_o^2 \frac{\partial \omega}{\partial p} \quad . \tag{6}$$

Here, $\frac{\delta}{\delta t}$ is the local change in a coordinate system moving with the vorticity maximum.

Application of the operator, $\frac{\delta}{\delta t}$, to (6) yields an expression for the rate at which the intensification rate varies in time as a consequence of changes occurring in the field of vertical motion:

$$\nabla^2 \frac{\delta}{\delta t} \left(\frac{\delta \phi}{\delta t}\right) \equiv \nabla^2 \frac{\delta \chi}{\delta t} = f_o^2 \frac{\delta}{\delta p} \left(\frac{\delta \omega}{\delta t}\right) \quad . \tag{7}$$

Temporal variations in the field of vertical motion result from changes occurring in each of the forcing functions of (4). Of interest in self-development are variations in the vertical motion over the low center and, therefore, in the

rate of surface development that result from changes in the field of vorticity advection.[4]

In order to evaluate the mechanisms which produce changes in the field of vertical motion by modifying the pattern of vorticity advection, the $\frac{\delta}{\delta t}$ operator is applied to the left-hand side and term (1) of (4). With the assumption that the stability factor, σ, is invariant in time, the resulting expression is

$$(\sigma\nabla^2 + f_o \frac{\partial^2}{\partial p^2}) \frac{\delta\omega}{\delta t} = f_o \frac{\partial}{\partial p} [\frac{\delta V}{\delta t} \cdot \overset{(A)}{\nabla}(\frac{1}{f_o} \nabla^2\phi + f)] + f_o \frac{\partial}{\partial p} [V\cdot\nabla \overset{(B)}{\frac{\delta}{\delta t}} (\frac{1}{f_o} \nabla^2\phi)] \quad . \qquad (8)$$

It can be seen from (8) that temporal variations in the field of vertical motion result from altering the advecting velocity, term A, and the gradient of relative vorticity, term B. Modification of each results from changes occurring in the field of geopotential, which can be obtained from solution of (4) and substitution of the results into (3).

---

[4]In a developing cyclone the Laplacian of thermal advection over the low center is characteristically small in magnitude (see e.g., Petterssen, 1956). Time variations in the pattern of thermal advection are therefore not likely to contribute significantly towards modifying the rate of development. On the other hand, although precipitation is typically absent from the center of storms in the initiation of cyclogenesis, the Laplacian of diabatic heating over the surface low need not necessarily be small. Temporal variation in the amount of rainfall being produced, for example, by a squall line along the cold front can therefore alter the rate of a storm's development. This effect, as true also for time variation in the pattern of thermal advection, is not conceptually included in the process of self-development and is not here a subject of investigation.

The values of $\frac{\delta\omega}{\delta t}$ obtained from (8) on the basis of the computed geopotential tendencies can then be utilized to evaluate the acceleration of the intensification rate, $\frac{\delta}{\delta t}(\chi)$, from (7). Note that one can obtain the separate contributions of vorticity advection, thermal advection, and diabatic heating to terms A and B of (8) and, therefore, the separate contributions of each to $\frac{\delta}{\delta t}(\chi)$ through the effects represented by terms A and B. Actually, the influence of term A is not specifically included in the concept of self-development, nor is the effect of vorticity advection on term B. The influence of each, however, is evaluated in this study. Figure 2 summarizes the mechanisms contributing to time changes of the intensification rate which are evaluated in this study.

B. MODEL AND PROCEDURES

The concepts just described for accessing the acceleration of the intensification rate were applied to a structurally simple analytic model of cyclonic and anticyclonic disturbances in the baroclinic westerlies and to a major cyclogenesis over the central United States, 10 December 1971. In solution of the relevant equations, a three-dimensional grid of data points is employed. The vertical grid array (Fig. 3) employs data at each 100 millibar level from 1000 to 100 mb. The horizontal grid measures 27 x 27 points with a grid interval of 160 km at 60° and 30°N on a Lambert Conic Projection

(see Fig. 3 for grid location). All derivatives are replaced by central finite differences, with the resulting set of algebraic equations solved by the Liebmann relaxation process. The boundary conditions are $\omega = 0$ and $\frac{\partial \omega}{\partial t} = 0$ at all lateral and vertical boundaries. The static stability factors utilized are those for the standard atmosphere as given in Table I. The standard value of the coriolis factor, f_o is that for 39°N, $.92 \times 10^{-4}$ sec^{-1}.

As shown in Fig. 5, subsequent to generating the three-dimensional fields of geopotential and heating, the first step in the computation procedure is to evaluate the contribution of the forcing functions in (4) to the field of vertical motion, ω. The respective contribution of each to the geopotential tendency is then computed via (3). Actually, two sets of tendencies for each forcing function are obtained; the first being that associated solely with the divergence $(\frac{\partial \omega}{\partial p})$ term of (3), while the second is the total tendency. The first set of tendencies relates to the developmental influence of each forcing function, while the second set includes the effects of development and motion.

Once the field of geopotential tendency is obtained, the influence of each contributing factor thereto upon $\frac{\delta \omega}{\delta t}$ is evaluated from (8). The separate contributions of terms A and B are determined. Finally, the respective influence of the relevant physical effects to temporal variations in the rate of development is ascertained from (7).

The forcing functions of (4) and , consequently, all which follows therefrom are specified by the three-dimensional field of geopotential and distribution of diabatic heating. Input for the real case study was height data at mandatory data levels (1000,850,700,500,400,300,200, and 100 mb), converted by quadratic fit where necessary to give ϕ at each 100 mb level. Analysis of the geopotential fields were accomplished by an objective technique known as HOBAN (Inman, 1970). HOBAN is basically a successive approximation scheme that starts with a large influence radii and reduces the radii on successive passes to give a more local fit on the last pass. The scheme makes use of height and wind within and outside a local limited area grid. The scheme employs a distance dependent weighting function following Cressman (1959). In an extensive evaluation of HOBAN, Stuart (1974) found the analyzed height field and quasi-geostrophic omegas derived therefrom compared quite favorably with the height and omega fields obtained from carefully prepared and consistent subjective analyses that were used as the basis for judgement. Analyses of the 1000 and 500 mb height fields on 1200 GMT 10 December 1971, the time for which computations are performed, are shown in Fig. 6 and 7, respectively.

In addition to the real data case, computations are performed for the structurally simple model of the geopotential and temperature fields of cyclonic and anticyclonic

disturbances, after Sanders (1971). At 1000 mb, the disturbances of geopotential is given analytically by

$$\phi(x,y,1000) = \hat{\phi}_{1000} \text{ Cos } \frac{2\pi}{L} (x+\lambda) \text{ Cos } \frac{2\pi}{L} y \ , \qquad (9)$$

where the x and y axes are directed eastward and northward, respectively; $\hat{\phi}_{1000}$ is the amplitude of the pressure perturbation; L is the horizontal wavelength; and λ is the phase lag of the 1000 mb geopotential field relative to the temperature field, which is specified by

$$T(x,y,p) = T_M(p) - (1 - \alpha \ln \frac{1000}{p})(ay + \hat{T} \text{Cos } \frac{2\pi}{L} x \text{ Cos } \frac{2\pi}{L} y) \ . \qquad (10)$$

Here, $T_M(p)$ is the mean temperature at the pressure level, p, "a" is the mean north-south temperature gradient, and $\hat{T}$ is the amplitude of the temperature perturbation. The vertical structure of the temperature perturbation is governed by the factor $(1 - \alpha \ln \frac{1000}{p})$, which allows for damping with elevation and reversal of sign at a pressure level determined by the value of α. With $\alpha = .722$, the temperature reversal and, hence, the simulated tropopause occur at the 250 mb level, as in middle-latitudes in the real atmosphere, while the strength of the temperature perturbation at 500 mb drops to one-half its 1000 mb value. Note that $\lambda = 0$ corresponds to a system of warm lows and warm highs. The 1000 mb pattern with $\lambda = L/2$ yields cold lows and warm highs. The 1000 mb

pattern with $\lambda = L/4$, representing the typical intensifying situation in the real atmosphere, and with model parameters obtained from the system of 1200 GMT 10 December 1971 is shown in Fig. 8.

At all levels above 1000 mb, the geopotential fields are obtained by hydrostatic integration; thus,

$$\phi(x,y,p) = \phi(x,y,1000) + \int_{1000}^{p} \frac{\partial \phi}{\partial p}(x,y,p)\, dp$$

$$= \phi_M(p) + \phi(x,y,1000) - \left[R \ln \frac{1000}{p} - \left(R \frac{\alpha}{2}\right)\left(\ln \frac{1000}{p}\right)^2\right]$$

$$x \left(ay + \hat{T} \operatorname{Cos} \frac{2\pi x}{L} \operatorname{Cos} \frac{2\pi y}{L}\right), \qquad (11)$$

where

$$\phi_M(p) = R \int_{p}^{1000} T_M(p)\, d \ln p \qquad (12)$$

The height field at 500 mb corresponding to the situation in Fig. 8 is presented in Fig. 9. It should be noted that Fig. 8 and Fig. 9 represent contour analyses of the grid point height values ascertained from the analytic expressions above. Further, all computations are performed on the 27 x 27 x 10 grid in the same fashion as for the real case.

The main contribution to diabatic heating is assumed to be from the heat released by condensation. Other heat sources and sinks are neglected. Furthermore, it is assumed that condensation occurs as liquid water which immediately falls out as precipitation.

For the real data case, precipitation rates at 1200 GMT 10 December 1971 were obtained from the observed two-hour amounts ending at 1300 GMT, subjectively averaged over 160 km^2 areas centered at grid points (Fig. 10). Area averaged precipitation rates were converted to the vertically integrated heating by multiplication with the latent heat factor, L. The vertical partitioning of the latent heat release is per the analytic model discussed below, with the level of maximum heating, 400 mb, consistent with the fact that the observed precipitation was primarily convective in nature.

In the analytically specified cyclonic system, the basic horizontal distribution of rainfall is modeled as an ellipse in which the maximum precipitation rate, P_M, is at the center and values of P decrease exponentially therefrom (after Tracton, 1973). Thus

$$p(x,y) = P_M \, e^{-[\frac{x^2}{A^2} + \frac{y^2}{B^2}]} ,$$

where A and B are scale factors which specify the major and minor axis (x and y, respectively) of the ellipse defined by $P(x,y) = .1 \, P_M$. The vertical distribution of heating is of the form

$$e^{-cz} \sin z , \qquad (13)$$

where

$$z = \left(\frac{p - p_1}{p_o - p_1} \right) \pi$$

p_o = 1000 mb

p_1 = 200 mb = level at which heating goes to zero ,

and c specifies the level of maximum heating.

Computation of all quantities are performed for four variations of the basic distribution of heating. The first, Case I, is that of an ellipse centered one grid to the east and one grid to the north of the 1000 mb low, with the value of A and B such that the major and minor axes are 1440 and 640 km respectively (Fig. 11). The value of "c" in this case is in accordance with the heating maximum in the vertical lying at 700 mb (Fig. 12). Motivation for the first case is to simulate the stratiform precipitation characteristically observed ahead of a low in advance of the warm front. The maximum intensity of heating at 700 mb is explained by large values of $\frac{dq_s}{dp}$ (q_s = saturation specific humidity) near the surface and large values of vertical motion near 500 mb. The correlation between ω and $\frac{dq_s}{dp}$, which determines the rate of stable precipitation, therefore tends to be largest somewhere between these levels.

The second case considered, Case II, is the same as the first, except that the level of maximum heating is specified as 400 mb (Figs. 11 and 12). Here, an attempt is made to simulate the effect of convection embedded in a warm-frontal

precipitation pattern. As noted by Tracton (1968), warm-front precipitation is largely produced by convective overturning, rather than by stable saturated ascent. Although little is known about the detailed distribution of latent heat release by cumulus convection, theoretical treatments of various investigations (e.g., Kuo, 1965; Kasahara and Asai, 1967) appear to agree that convective heating is largest in the middle to upper troposphere; hence, the choice of 400 mb for Case II.

The third variation of heating for which computations are performed, Case III, is that of an elongated ellipse, 1440 x 320 km, centered one grid distance to the east and one grid distance to the south of the 1000 mb low and oriented 45° from the north-south direction (Fig. 13). Motivation in this case is to simulate the influence of a squall line along or just ahead of the cold front. Squall-line precipitation is, of course, convectively produced and, hence, the level of maximum heating is specified to be at 400 mb.

The final case examined, Case IV, represents a superposition of the squall line (Case III) and the stratiform, warm frontal precipitation pattern (Case I).

Note that in all cases, P_M is specified to have the synoptically reasonable value of .5 in hr^{-1}.

III. RESULTS AND DISCUSSION

A. ANALYTIC MODEL CASES

Table II presents the tendencies at the 900 mb low center.[5] The tendencies are, of course, a measure of the instantaneous rate of low-level development but are presented in synoptically familiar terms of change in central pressure per hour. Note that the tendencies associated with vorticity advection, χ_1, and thermal advection, χ_2, are independent of the diabatic heating, χ_3, and, therefore, the same for each of the cases considered.

Exclusive of the influence of latent heat release, it is clear from Table II that vorticity advection is the dominant process contributing to development, i.e., the active deepening mechanism. Thermal advection, in accord with the qualitative arguments of Petterssen (1956), produces pressure falls in advance and rises to the rear of a cyclone, but has very little effect at the low center itself (Fig. 15). The deepening produced by vorticity advection, -.63 mb hr^{-1}, is consistent with the value obtained by Sanders (1971).

The influence of latent heat release upon the deepening rate varies according to the distribution of the heating with respect to the low center. Values range from -.55 mb hr^{-1} in

---

[5]The 900 mb level is the lowest one for which tendencies are explicitly computed. Tendencies at 1000 mb required for boundary values in solution of (8) are obtained by quadratic interpolation.

the squall line simulation (Case III) to -2.36 mb hr^{-1} in the case where the level of maximum heating associated with warm frontal precipitation is at 700 mb (Case I). Of course, in each of the cases considered a shift in the location of the center of heaviest precipitation would affect the magnitude of the computed influence of heating upon the deepening rate. Translation of the maximum in precipitation rate to the low center, as is characteristic of the initial stages of cyclogenesis (Tracton, 1973), would result in increasing the influence of condensational heating upon the instantaneous rate of development (e.g., see Fig. 16). Note also that the magnitude of the tendencies associated with heating are proportional to the specified values of P_M, which in all the above cases is .5 in hr^{-1}.

Values of the computed time rate of change in intensification rates at the 900 mb low center appear in Tables III and IV. The results presented in Table III are based upon geopotential tendencies associated with only the divergence term of (3), while Table IV reflects the field of total tendency produced by each forcing function. Reference should be made to Fig. 2 for the meaning of terms in Tables III and IV. Note that calculated values of the instantaneous acceleration of the intensification rate have been applied to 12 hour periods for ease in interpreting the results.

The terms which specifically relate to the process of self-development are $\frac{\partial \chi_{2B}}{\partial t}$ and $\frac{\partial \chi_{3B}}{\partial t}$. The former reflects

the influence of thermal advection upon the gradient of relative vorticity and, hence, vorticity advection over the storm center, while the latter represents the effect upon the gradient of relative vorticity resulting from diabatic heating. Table III indicates that the thermal advection effect produces an increase in the deepening rate of .46 mb hr^{-1} per 12 hr. This corresponds to an increase of 75 per cent in the rate of development associated with the field of vorticity advection. The physical mechanisms which are operative here are illustrated in Figs. 17 to 19. In response to the pattern of thermal advection (Fig. 17), height rises occur aloft in advance of the surface low, while height falls occur aloft behind the low position (Fig. 18). The height rises and falls correspond to generation of anti-cyclonic and cyclonic vorticity, respectively. The enhanced variation of vorticity and resultant increase in vorticity advection along the upper current over the surface low intensifies the vertical motion over the low (Fig. 19). The consequent increase in low-level convergence then results in an increased rate of development.

The influence of latent heat release in self-development, as shown in Table III, ranges from -.002 to -.50 mb hr^{-1} per 12 hr. The smallest effect occurs in the squall line simulation (Case III). This reflects the fact that the height changes induced aloft by the heating result in an increased gradient of vorticity across, rather than along the upper flow. Hence, the field of vorticity advection

over the low is not significantly altered. In addition, as can be seen in Fig. 19, the impact of the heating upon the vertical motion is principally at levels above 700 mb. Consequently the effect of heating upon the low-level convergence and, therefore, upon self-development is minimal.

The largest impact of latent heat release occurs in the 700 mb warm front precipitation and in the combination 700 mb warm frontal and squall-line precipitation case (Cases I and IV, respectively). Note that the computed acceleration of the intensification rate, -.50 mb hr^{-1} per 12 hr in both cases, is comparable in value to that ascertained for thermal advection. Here, the upper level height rises induced by the heating (Figs. 20 and 21) tend to amplify the ridge downstream from the low center, such that the enhanced vorticity advection over the low results in an increased rate of intensification. The lesser effect (-.035 mb hr^{-1} per 12 hr) when the level of maximum heating is at 400 mb, rather than 700 mb, results from the shift upward of the level at which heating has its greatest influence on the vertical motion. The impact of the heating in Case IV is simply not felt at low levels.

Recall that the motivation for the 400 mb warm frontal precipitation case was to simulate the effect of convection embedded in large-scale stratiform precipitation, which alone would have a level of maximum heating around 700 mb. Actually, in most instances, said convection does not extend above the

400 to 500 mb level (Tracton, 1968), so that the effective level of maximum heating would likely lie somewhere between 700 and 400 mb. The total range of values of $\frac{\partial \chi_{3B}}{\partial t}$ for warm frontal precipitation is thus -.50 to -.035 mb hr^{-1} per 12 hr. While the apparent influence of convection is to reduce the effect of heating upon self-development through raising the level of maximum heating, it should be noted that the maximum in the rainfall rate (to which all computed quantities are proportional) is likely greater in the case of convection embedded in stratiform precipitation than when the precipitation is purely stratiform. In addition, the horizontal scale of heating is less in convective situations, so that through the influence of the Laplacian in the relevant equations, the importance of heating would be greater.

With reference again to Case IV, note that, although the combined maximum precipitation rate is somewhat greater than that of Case I (Fig. 14 and 11, respectively), the effect of heating on self-development is exactly the same. This reflects the offsetting influence of an effective rise in the level of maximum heating and the shift in the location of the center of precipitation with respect to the low center.

From Table III it can be seen that the effect of vorticity advection upon the gradient of vorticity and, therefore, upon the field of vorticity advection itself $(\frac{\partial \chi_{1B}}{\partial t})$, is to produce an increase of .22 mb hr^{-1} per 12 hr in

the rate of development. As stated previously, this mechanism is not conceptually included in self-development. The effects of thermal advection, vorticity advection, and heating upon the pattern of vorticity advection through their influence upon the advecting velocity (all "A" terms) can be seen from Table III to be negligible. These effects are also not specifically encompassed in self-development.

It can be seen from Table IV that the $\frac{\partial \chi}{\partial t}$'s computed on the basis of the total tendency produced by each forcing function are either negligible in value or positive in sign. Thus, for example, the thermal advection effect, $\frac{\partial \chi_{2B}}{\partial t}$, produces a decrease in the deepening rate of .73 mb hr^{-1} per 12 hr, rather than the previously discussed increase of .46 mb hr^{-1} per 12 hr. The apparent reason for this is that the structure of the analytical model is such that the maximum in the field of vorticity advection lies ahead of the surface low position (Fig. 22). Consequently, when one includes the vorticity advection term of (3) into the computed tendencies, the induced translation of the upper trough eastward results in smaller values of vorticity advection becoming superimposed over the surface low.[6] The resultant reduced rate of low-level development (.73-(-.46) = 1.19 mb hr^{-1} per 12 hr) is then sufficien to offset the opposing influence of the

---

[6]The speed of translation of the upper trough is greater than that of the surface low (Sanders, 1971).

the developmental components of the forcing functions. It should be noted that the situation here is similar to that of a cyclone in the occluding (but not fully occluded) stage of its life history. In an earlier stage of development, when the maximum of vorticity aloft lies to the rear of the storm center, the effect of translation would be to progressively increase the rate of development. If the influence of translation in such a case were of the same magnitude as here, this process would dominate the individual contributions to self-development.

B. CASE OF 1200 GMT 10 DECEMBER 1971

The synoptic case is that of a developing frontal cyclone over the central United States on 10 December 1971 (Fig. 6). The initial development of the storm occurred around 0000 GMT 10 December over southeastern Oklahoma in association with an outbreak of convective showers in the vicinity of the low center (Fig. 23). By 1200 GMT, the convection began to spread eastward away from the center of the storm as the low continued to intensify and move northeastward toward the Great Lakes. This association between the initiation of cyclogenesis and convective activity, and the subsequent dissociation of the convection from the low center has been noted by Tracton (1973) to be characteristic of approximately one-half the cases of major cyclogenesis over the eastern two-thirds of the United States.

Figure 24 presents a plot of the observed change in central pressure versus time for the period 0000 GMT 10 December to 0000 GMT 11 December 1971. The 12-hour average deepening rate at 1200 GMT 10 December, the time for which computations are performed, is 1.08 mb hr^{-1}. The increase in the rate of development which is occurring at this time is 1.67 mb hr^{-1} per 12 hr.

Before presenting the results for the real data case, a few comments are in order with regard to their reliability. Although the contour analysis produced by the HOBAN scheme at each level appear synoptically acceptable (as, for example, Fig. 7) and are generally compatible with the corresponding NMC analyses, the vertical consistency between levels is somewhat dubious. This is apparent from the irregularities in the derived 1000-500 mb thickness pattern (Fig. 25). Adjustments to the HOBAN scheme, which are beyond the scope of this investigation, will be required in order to resolve the problem. In addition, Stuart (1974) noted that HOBAN does well on the general pattern and magnitude of main centers, but not so well on their precise location. In the case under study here, this is manifest in placement of the center of maximum vorticity advection ahead of the low rather than behind it, as is true in the NMC analysis and is implied by the observed increase in intensification rate.

With the above reservations, Tables II, III and IV present the computed tendencies and accelerations of the tendency at the 900 mb low center. The vorticity advection,

Table II, accounts for deepening at the rate of -.66 mb hr^{-1}, but this is largely offset by the thermal advection term whose magnitude is .56 mb hr^{-1}. HOBAN analyses do, in fact, show cold advection at low levels over the surface low. This, in itself, is not surprising in view of the asymmetrical nature of the system in question; however, there is little or no temperature advection (e.g., at 850 mb) in the corresponding NMC analysis. Table II indicates that diabatic heating contributes negligibly to the deepening rate, for the maximum of the precipitation pattern is too far removed from the low center to contribute directly to its development. The total computed tendency (-.12 mb hr^{-1}) is clearly inadequate to account for the magnitude of development which is observed.

From Table III one can see that thermal advection contributes -.43 mb hr^{-1} per 12 hr to the deepening rate through its influence upon the gradient of vorticity ($\frac{\partial \chi_{2B}}{\partial t}$); divergent effect only). Heating contributes negligibly to same, ($\frac{\partial \chi_{3B}}{\partial t}$), while the vorticity advection, which is not specifically incorporated in self-development, produces an acceleration in the tendency of -.43 mb hr^{-1} per 12 hr.

The combined effect of the thermal and vorticity advection upon changes in the deepening rate account for about one-half the observed acceleration; however, one can see from Table III that the remaining non self-development terms considerably offset their influence.

Note from Table IV that inclusion of the vorticity advection term into the tendencies required for computing acceleration of the intensification rate renders all computed values positive. That is, all effects contribute to decreasing the rate of development. This stems from the erroneous placement by the HOBAN scheme of the maximum of vorticity advection ahead, rather than behind the low center.

IV. SUMMARY AND CONCLUSIONS

The objective of this investigation was to assess quantitatively the process of self-development. Computations of relevant quantities within the framework of the quasi-geostrophic equations were performed on a real data case and an analytic specification of a cyclonic disturbance for which varying horizontal and vertical distributions of latent heat release were prescribed.

The quantitative reliability of the results obtained for the real data case are dubious because of apparent problems in the objective analysis scheme, HOBAN. Clearly, future effort should be directed towards remedying, if possible, the difficulties in HOBAN, so that the concepts and procedures described herein might be more reliably applied to real data case studies.

Results of computations utilizing the analytic model indicate that when only the divergence (i.e., development) term of (3) is utilized in determination of the fields of geopotential tendency required for determination of the $\frac{\partial \chi}{\partial t}$'s, the effect of latent heat release in self-development $(\frac{\partial \chi_{3B}}{\partial t})$ can be comparable with that of thermal advection. Specifically, in both the 700 mb warm frontal precipitation case (Case I) and the combined 700 mb warm frontal and squall line precipitation case (Case IV), the computed time rate

of change in deepening rate due to condensational heating was -.50 mb hr^{-1} per 12 hr, versus -.43 mb hr^{-1} per 12 hr due to thermal advection. In light of characteristically observed accelerations of intensification rate, as, for example, the -1.66 mb hr^{-1} per 12 hr for the 10 December 1971 case, the contribution of each mechanisms is considered synoptically significant, and their simultaneous occurrence even more so.

When the vorticity advection term of (3) is included in determination of the fields of geopotential tendency induced by the respective forcing mechanisms, the resulting $\frac{\partial \chi}{\partial t}$'s indicate a decrease, rather than an increase in the rate of development. This stems from the fact that the maximum of vorticity advection in the model lies ahead, rather than behind, the 1000-mb low center, which is contrary to the situation in the real atmosphere in association with a progressively intensifying cyclone. The magnitude of this effect, which represents translation of the vorticity maximum aloft with respect to the surface system, is 1.19 mb hr^{-1} per 12 hr. Clearly, if the magnitude of this influence were the same for the situation where the maximum of vorticity is approaching a surface cyclone, it would be the dominant mechanism contributing to intensification of the rate of development.

Note that the influence of heating is dependent upon the intensity and three-dimensional distribution of precipitation.

In this study, the intensity and distribution are synoptically and physically reasonable but, nevertheless, somewhat arbitrary. The same is true for all the structural parameters of the model, such as wavelength, intensity of the temperature perturbation, etc. Further experimentation with the model is therefore in order to generalize the results over a wide spectrum of situations. Finally, the concepts and approach employed here can be an important tool in diagnosing the performance of numerical prediction models in predicting extratropical cyclogenesis.

APPENDIX A

	900	800	700	600	500	400	300	200	100 mb
σ	.944	1.178	1.259	2.015	3.131	4.252	11.078	44.664	205.58

Table I. Stability Values, $\sigma(m^3 cb^{-1} TON^{-1})$

	CASE I	CASE II	CASE III	CASE IV	1200 GMT 10 Dec. 1971
X_T	- 3.00	-1.79	-1.19	- 2.85	- .122
X_1	- .63	- .63	- .63	- .63	- .66
X_2	- .01	- .01	- .01	- .01	.56
X_3	- 2.36	-1.15	- .55	- 2.21	- .022

Table II. Geopotential tendency at 900 mb low center.
Units: mb hr^{-1} (- = deepening, + = filling)

	CASE I	CASE II	CASE III	CASE IV	1200GMT 10 Dec.1971
$\frac{\partial X}{\partial t}_T$ A+B	-.95	-.606	-.624	-.96	-.401
A	.23	.109	.058	.22	.494
B	-1.18	-.715	-.682	-1.18	-.895
$\frac{\partial X}{\partial t}_1$ A+B	-.23	-.23	-.23	-.23	-.204
A	-.01	-.01	-.01	-.01	.239
B	-.22	-.22	-.22	-.22	-.443
$\frac{\partial X}{\partial t}_2$ A+B	-.38	-.38	-.38	-.38	-.173
A	.08	.08	.08	.08	.253
B	-.46	-.46	-.46	-.46	-.426
$\frac{\partial X}{\partial t}_3$ A+B	-.34	.004	-.014	-.35	-.0262
A	.16	.039	-.012	.15	-.002
B	-.50	-.035	-.002	-.50	-.026

Table III. Time rate of change of tendency derived from divergence term of (3). Units: mb hr^{-1}
(- = increase in deepening rate)

	CASE I	CASE II	CASE III	CASE IV	1200 GMT 10 Dec.1971
$\frac{\partial X}{\partial t}_T$ A+B	2.64	2.98	2.96	2.63	2.86
A	.25	.12	.07	.24	.22
B	2.39	2.86	2.89	2.39	2.64
$\frac{\partial X}{\partial t}_1$ A+B	.96	.96	.96	.96	.92
A	-.01	-.01	-.01	-.01	.15
B	.97	.97	.97	.97	.77
$\frac{\partial X}{\partial t}_2$ A+B	.82	.82	.82	.82	.95
A	.09	.09	.09	.09	.15
B	.73	.73	.73	.73	.80
$\frac{\partial X}{\partial t}_3$ A+B	.86	1.20	1.18	.85	.99
A	.17	.04	-.01	.16	-.08
B	.69	1.16	1.19	.69	1.07

Table IV. Time rate of change of tendency derived from divergence and vorticity advection terms of (3). Units: mb hr^{-1} per 12 hr (- = increase of deepening rate)

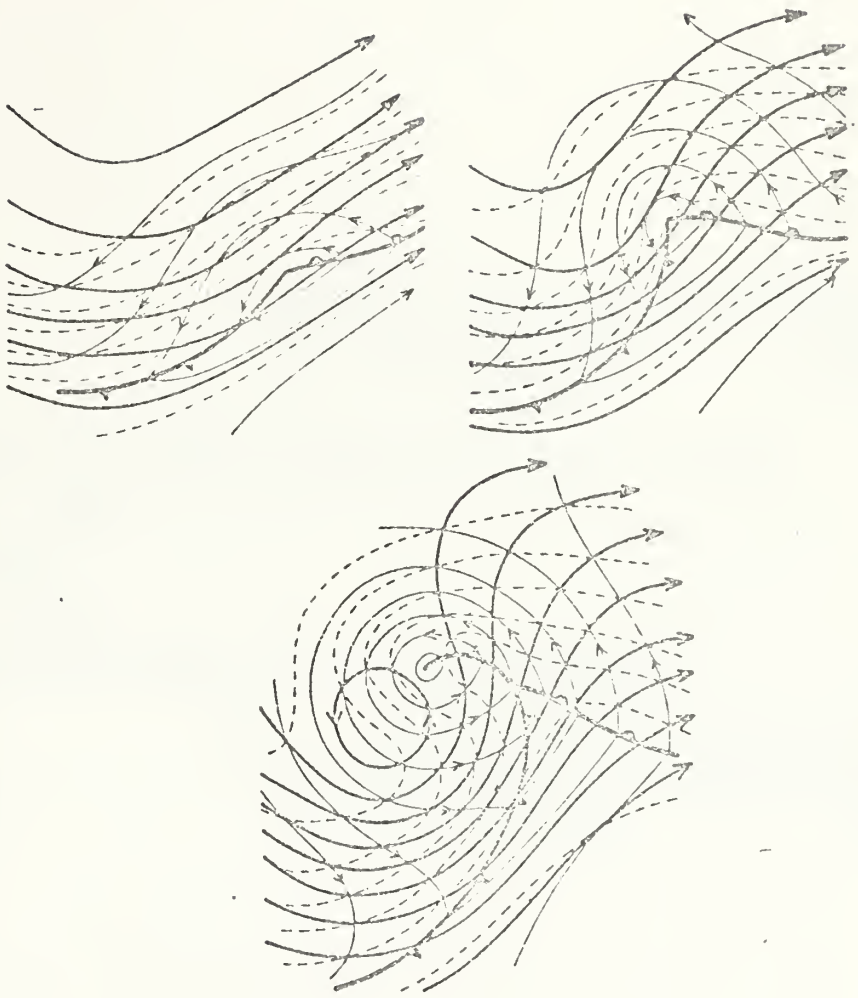

Figure 1. Schematic 500-mb contours (heavy solid lines), 1000-mb contours (thin lines), and 1000-500 mb thickness (dashed), illustrating the "self-development" process during growth of a cyclone. Thermal advection (geostrophic) of the 1000-500 mb layer is inversely proportional to the size of quadrilaterals formed by the 1000 mb contours and 1000-500 mb thickness lines (after Palmen and Newton, 1969).

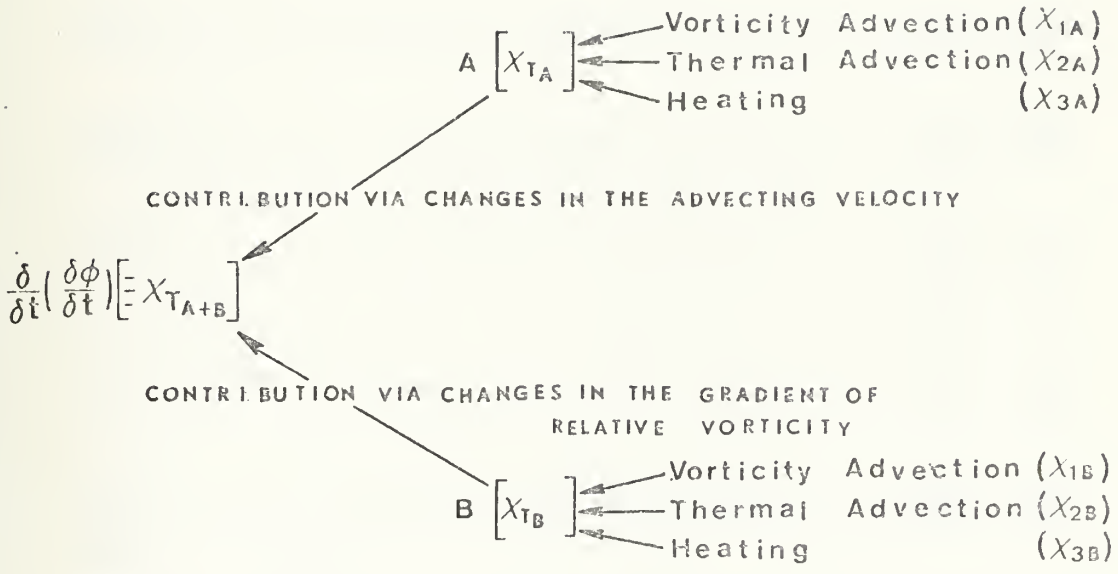

Figure 2. Summary of contributing factors to time changes of the intensification rate; note that χ_{2B} and χ_{3B} are the only effects specifically encompassed in self-development.

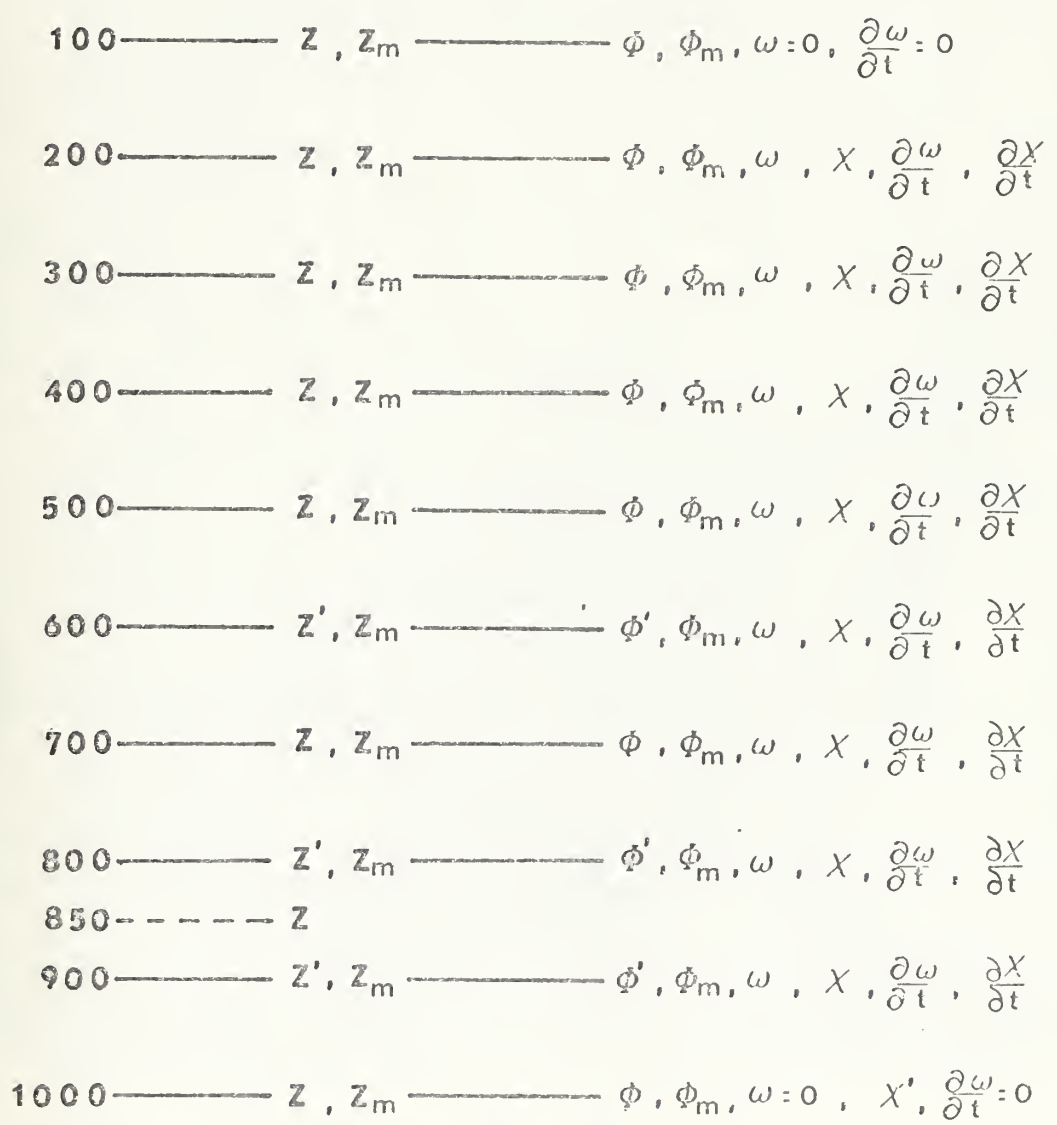

Figure 3. Vertical grid, prime quantities are obtained by quadratic interpolation from data at mandatory levels in case of Z' and ϕ', and from levels where quantities are explicitly evaluated in case of X', subscript "m" refers to analytic specification of initial fields.

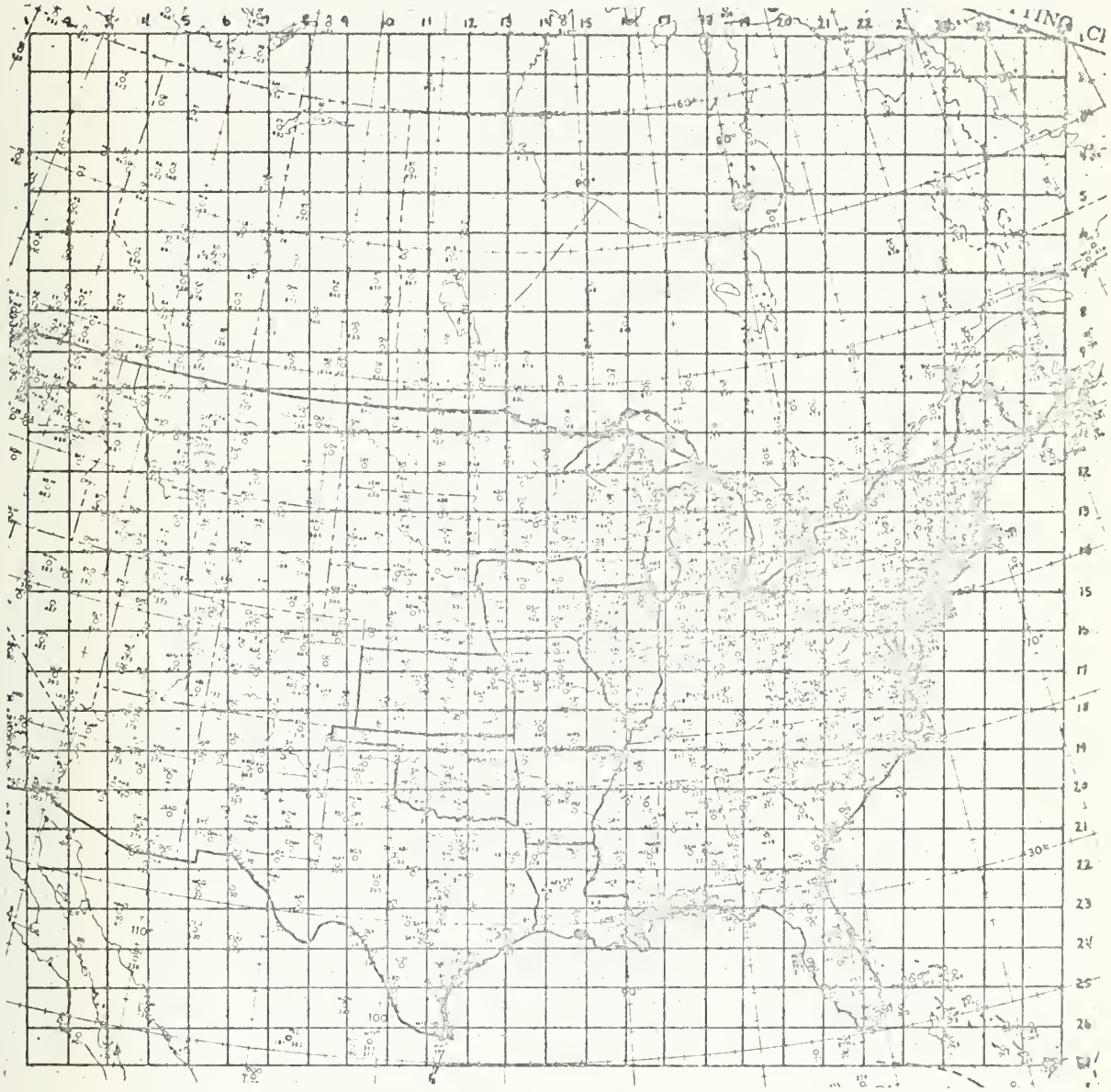

Figure 4. Placement of horizontal 27 x 27 grid.

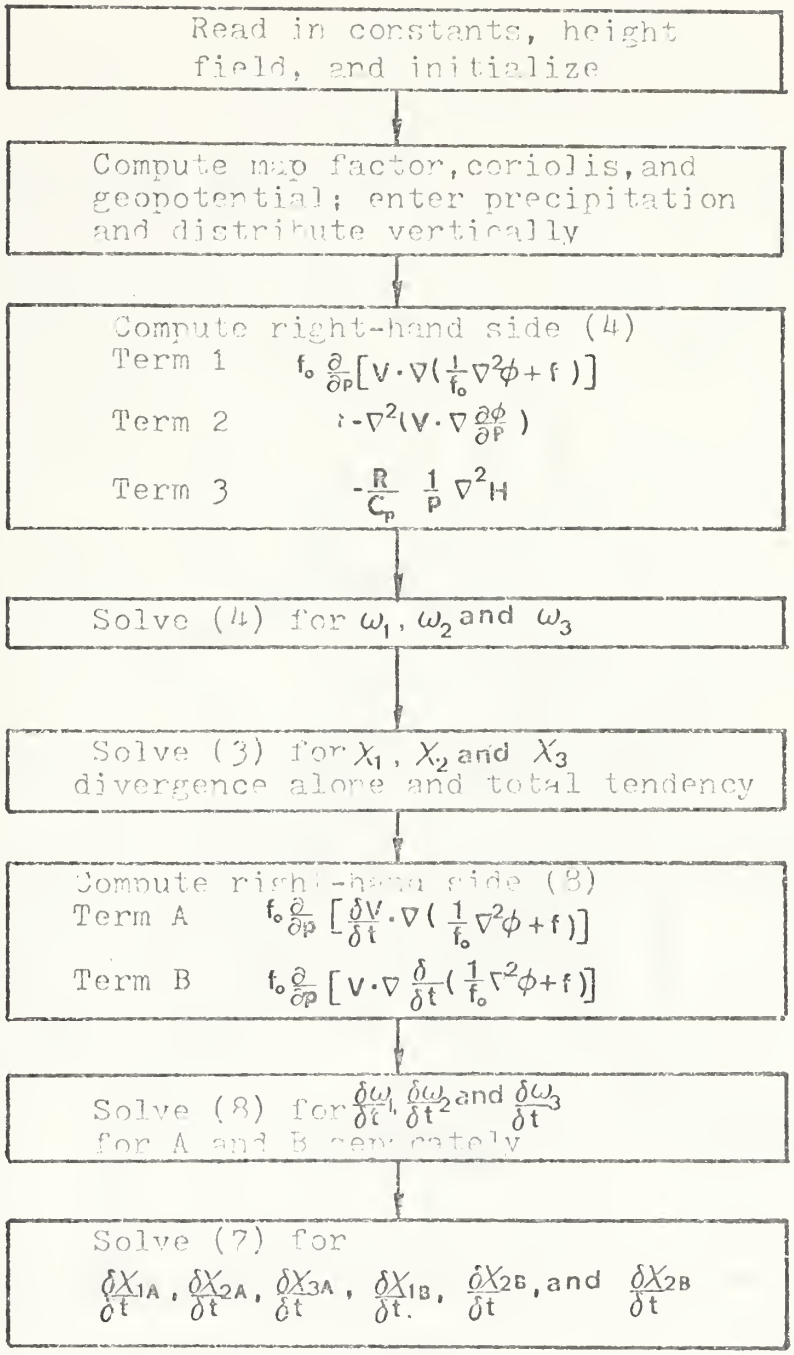

Figure 5. Schematic illustration of computation procedure

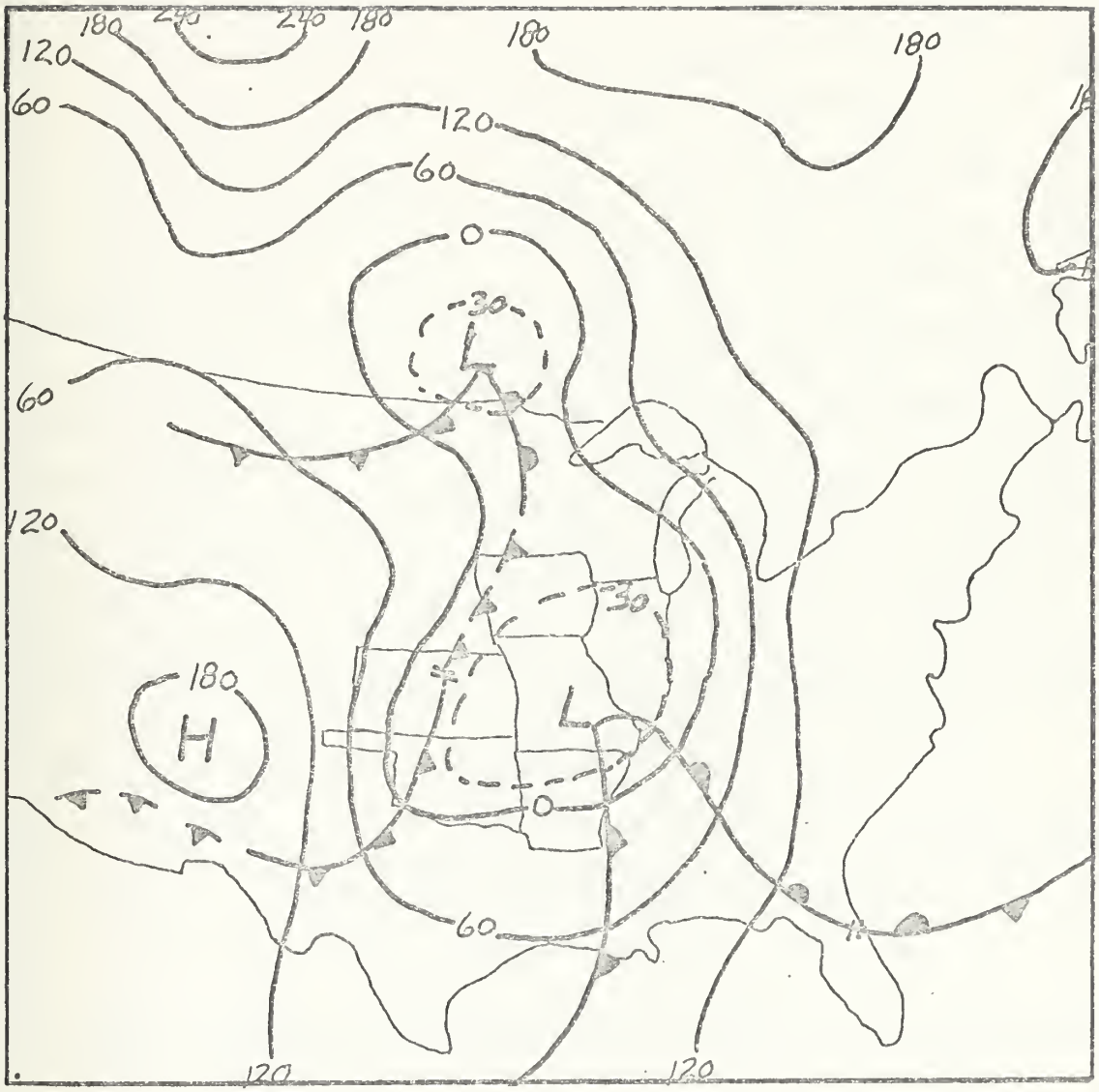

Figure 6. HOBAN generated 1000 mb height field for 1200 GMT 10 December 1971. (NMC frontal analysis superimposed). Units: m.

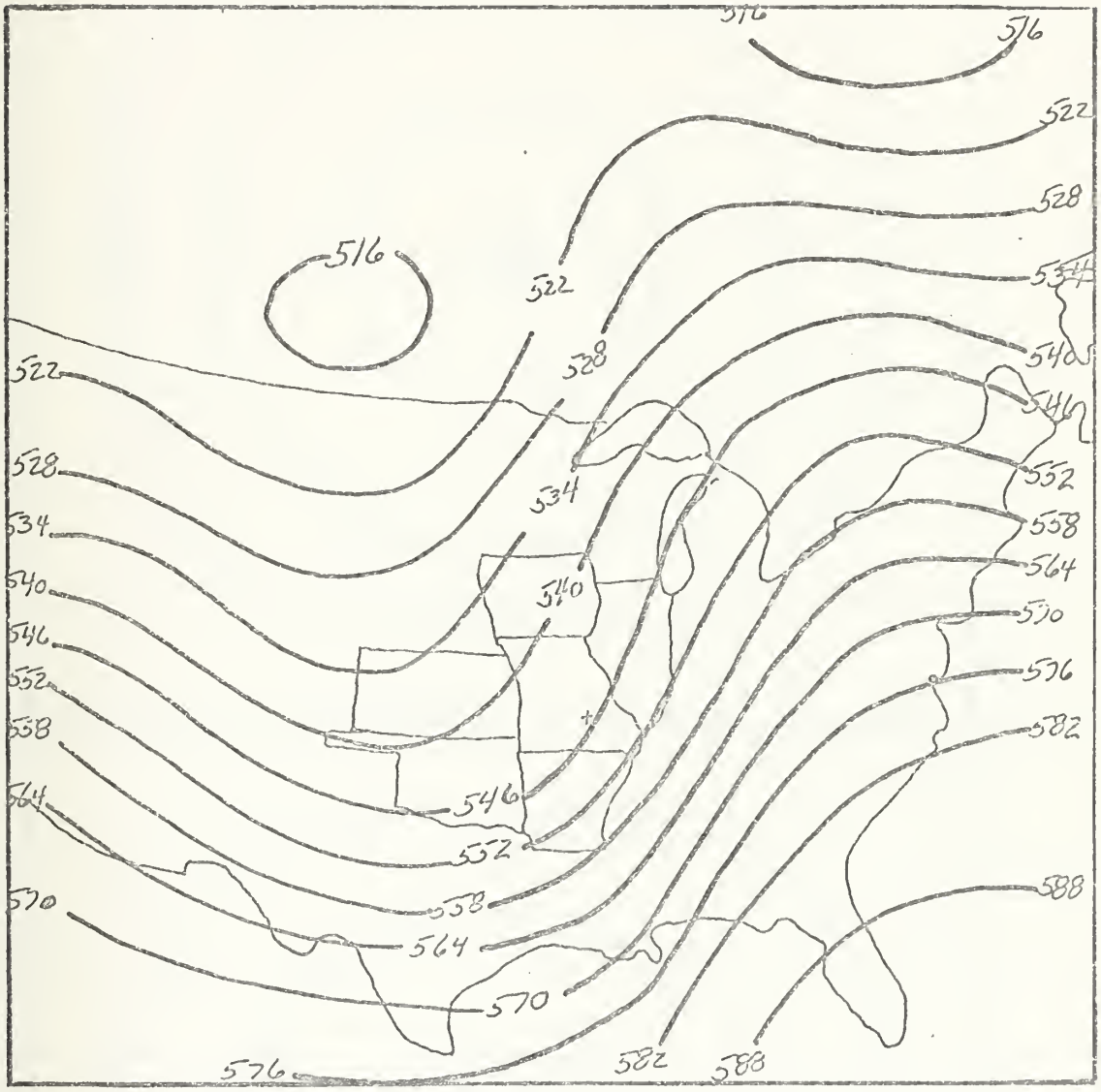

Figure 7. HOBAN generated 500 mb height field for 1200 GMT 10 December 1971 (+ indicates 1000 mb low position). Units: dm.

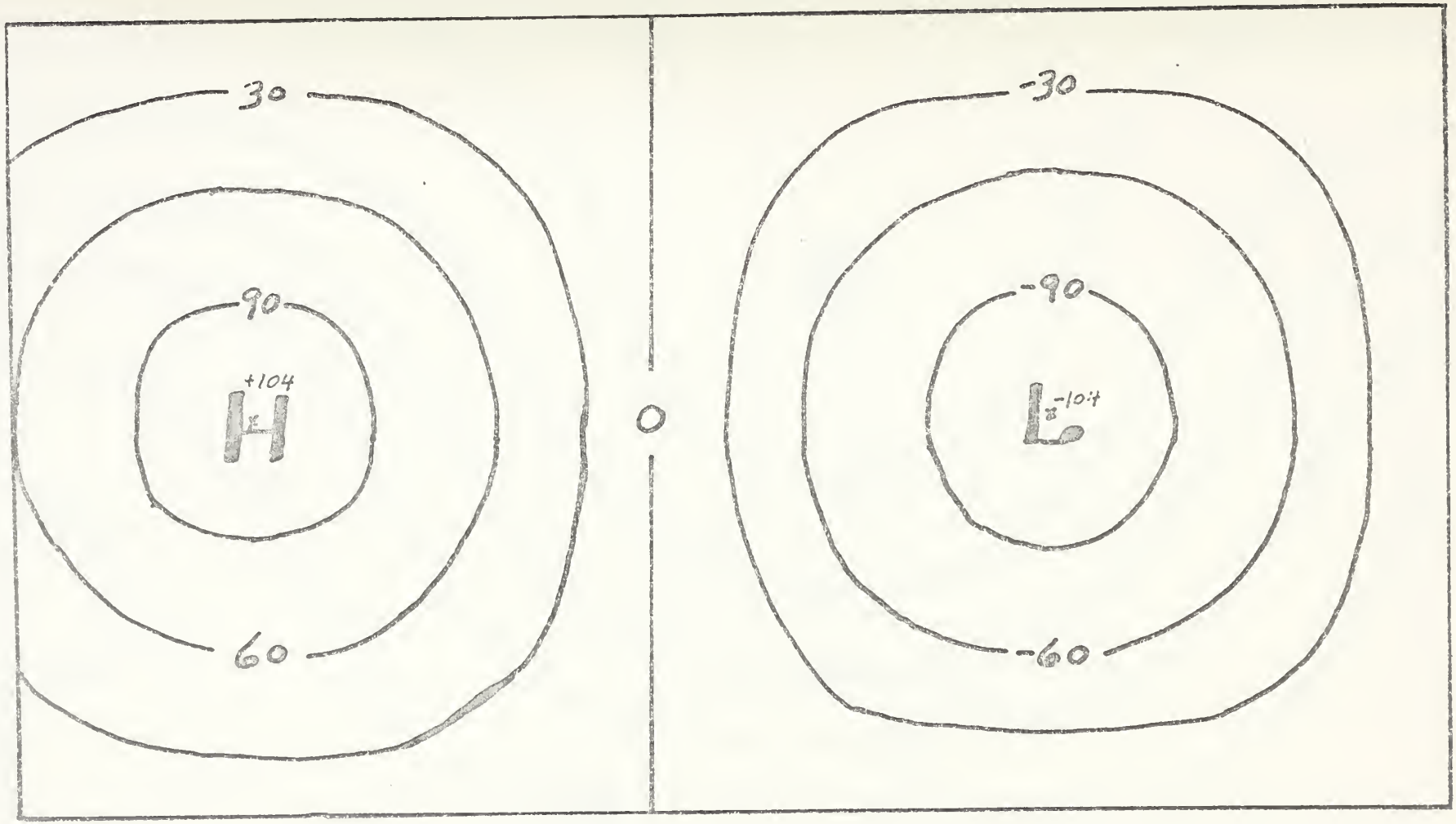

Figure 8. Analytic 1000 mb height field. (L = 3200 km, α = .722, $\hat{T}$ = 7.25°K, $a = 1.12 \times 10^{-5}$°Km^{-1}, $\hat{\phi}_{1000} = 1020\ m^2 sec^2$). Units: m.

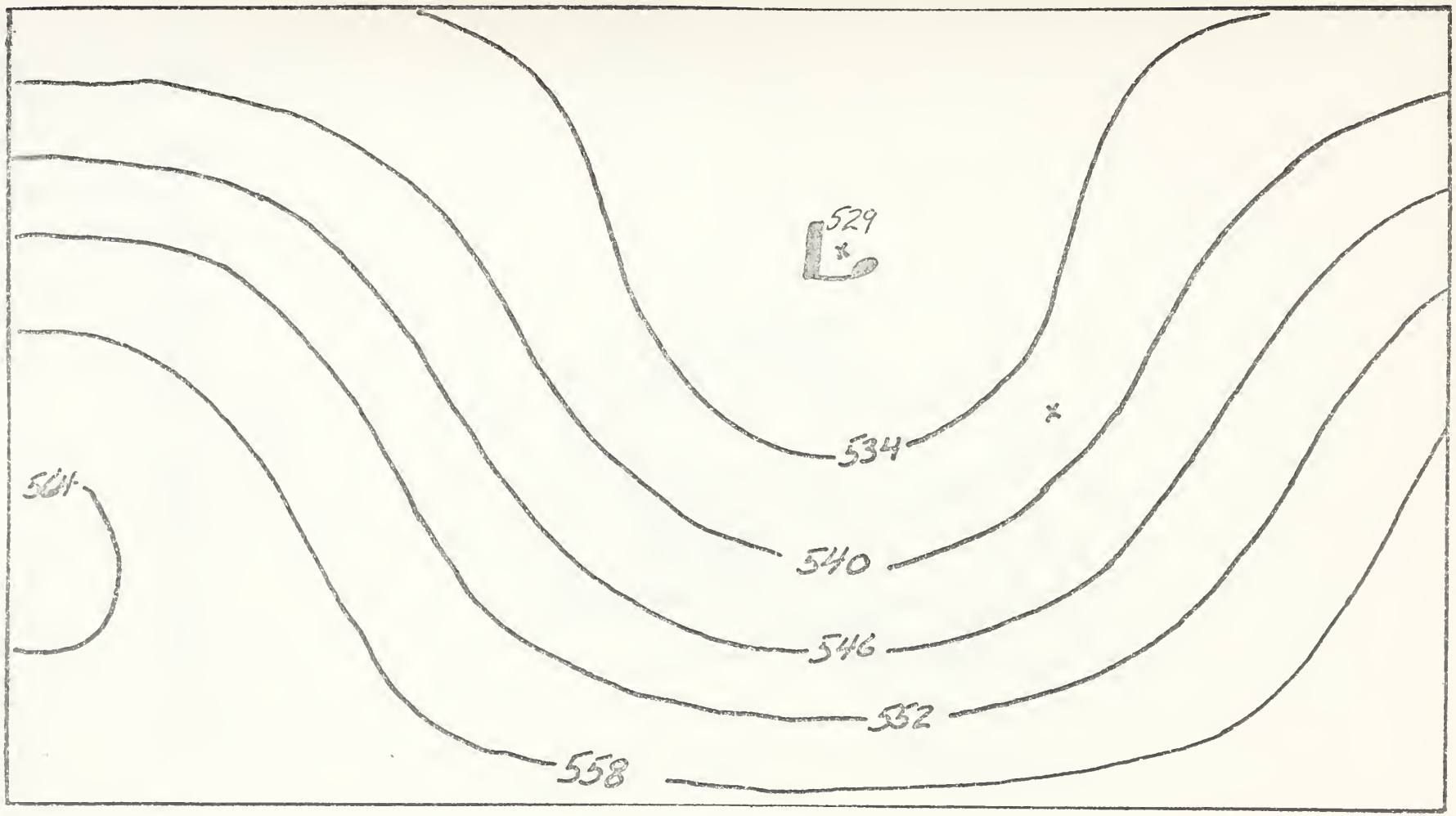

Figure 9. Analytic 500 mb height field (+ indicates 1000 mb low position). Units: dm.

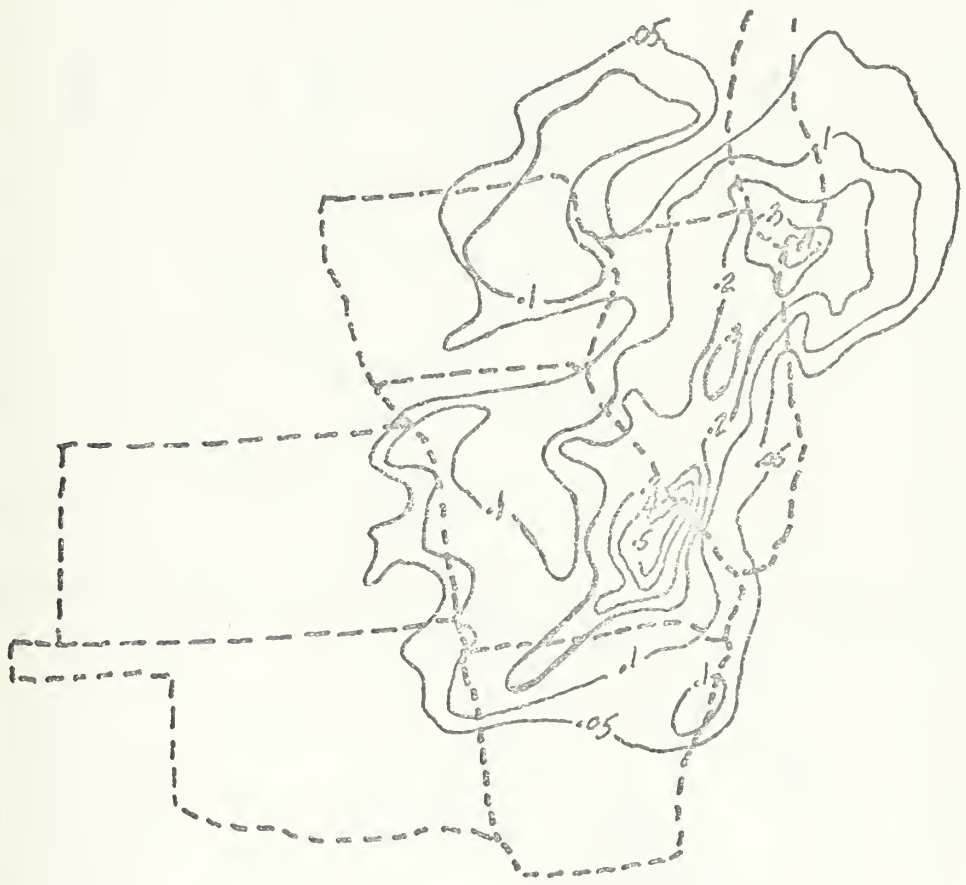

Figure 10. Observed rate of precipitation 1200 GMT 10 December 1971. Units: in hr^{-1}.

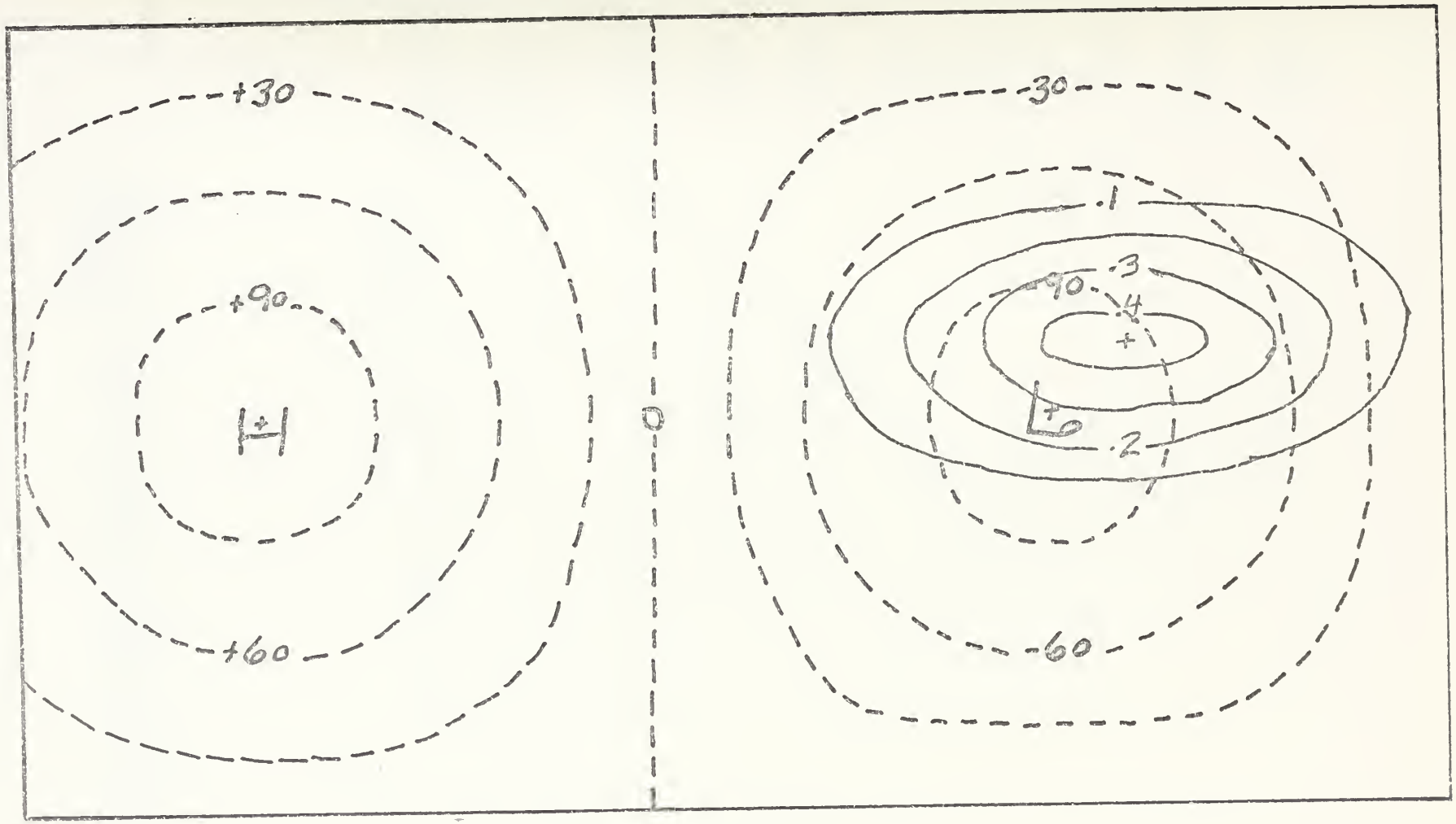

Figure 11. Surface precipitation pattern for analytical Cases I and II. Units: in hr^{-1}.

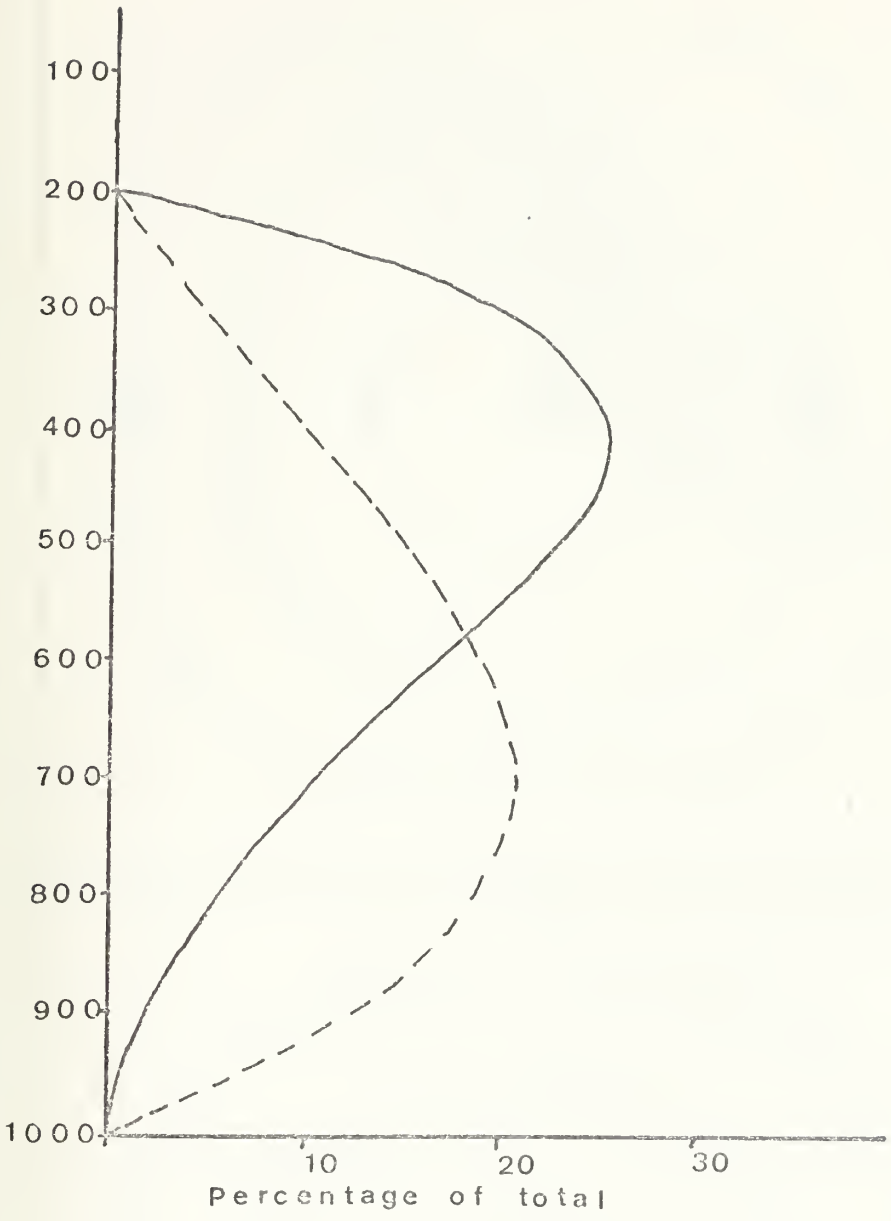

Figure 12. Vertical distribution of heating; solid line represents heating maximum centered at 400 mb and dashed line represents heating maximum at 700 mb.

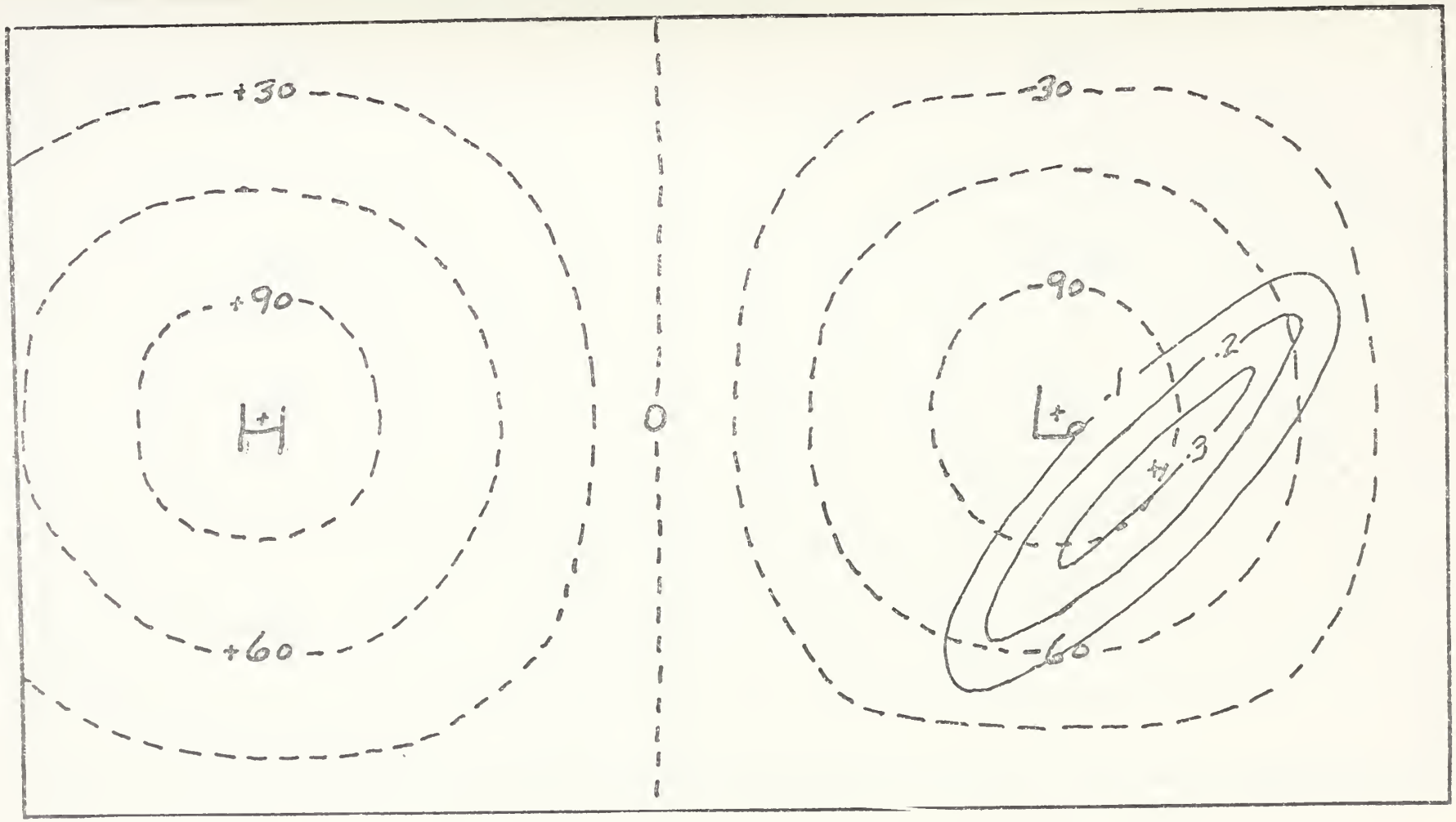

Figure 13. Surface precipitation pattern for analytic Case III
Units: in hr^{-1}

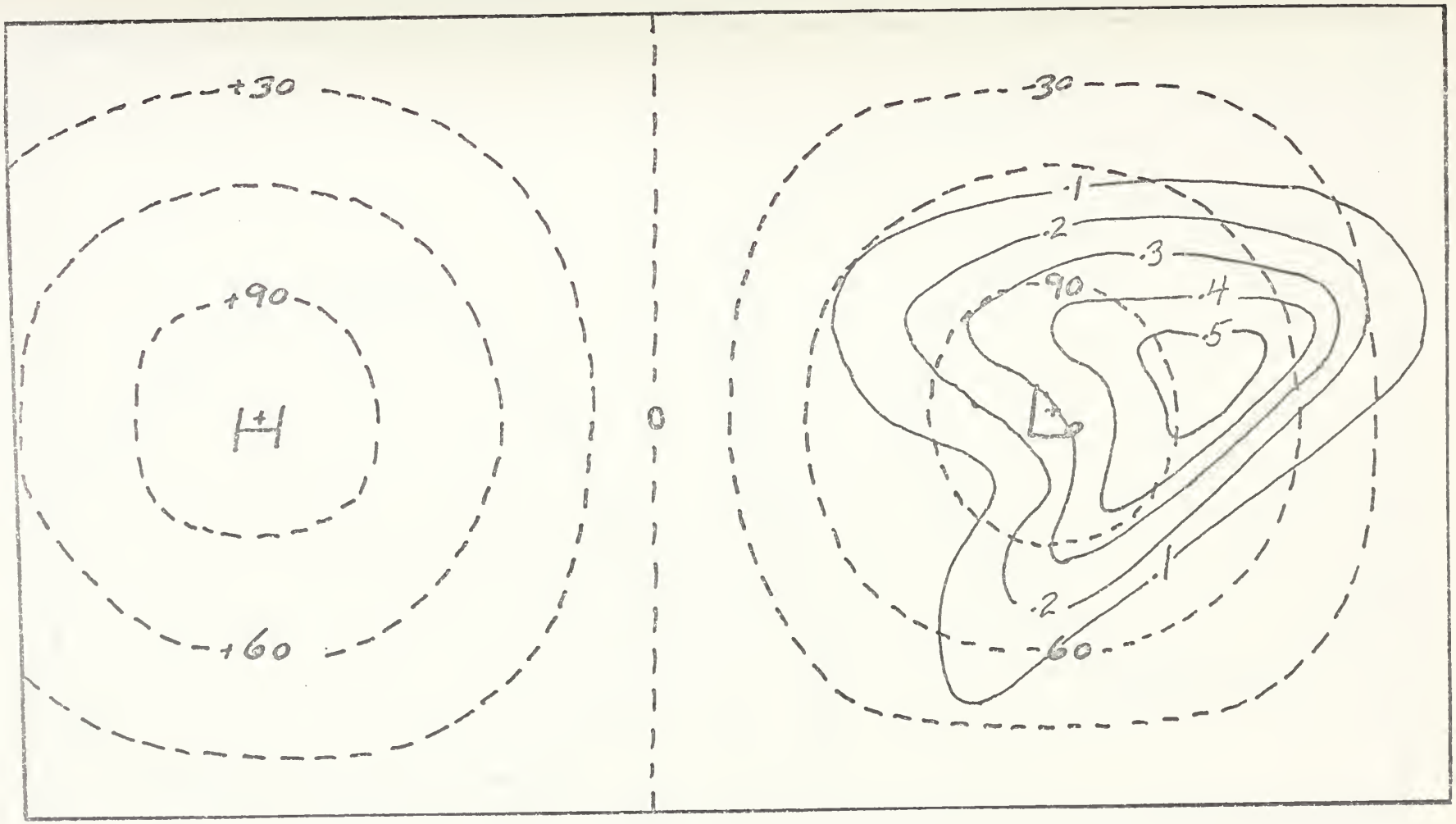

Figure 14. Surface precipitation pattern for analytic Case IV
Units: in hr^{-1}

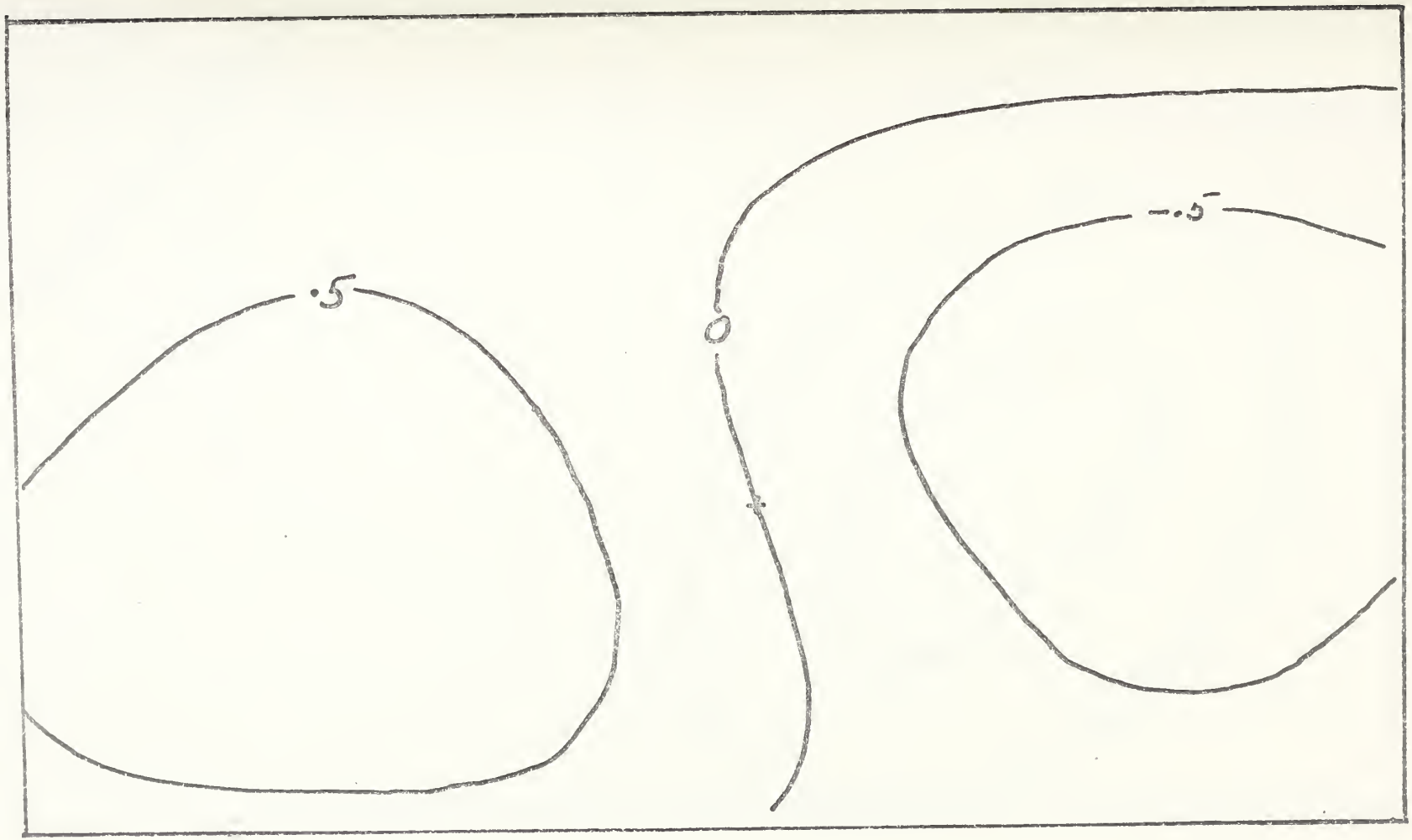

Figure 15. 900 mb thermal advection produced tendency (X_2)
Units: mb hr^{-1} (+ indicates position of 900 mb low center

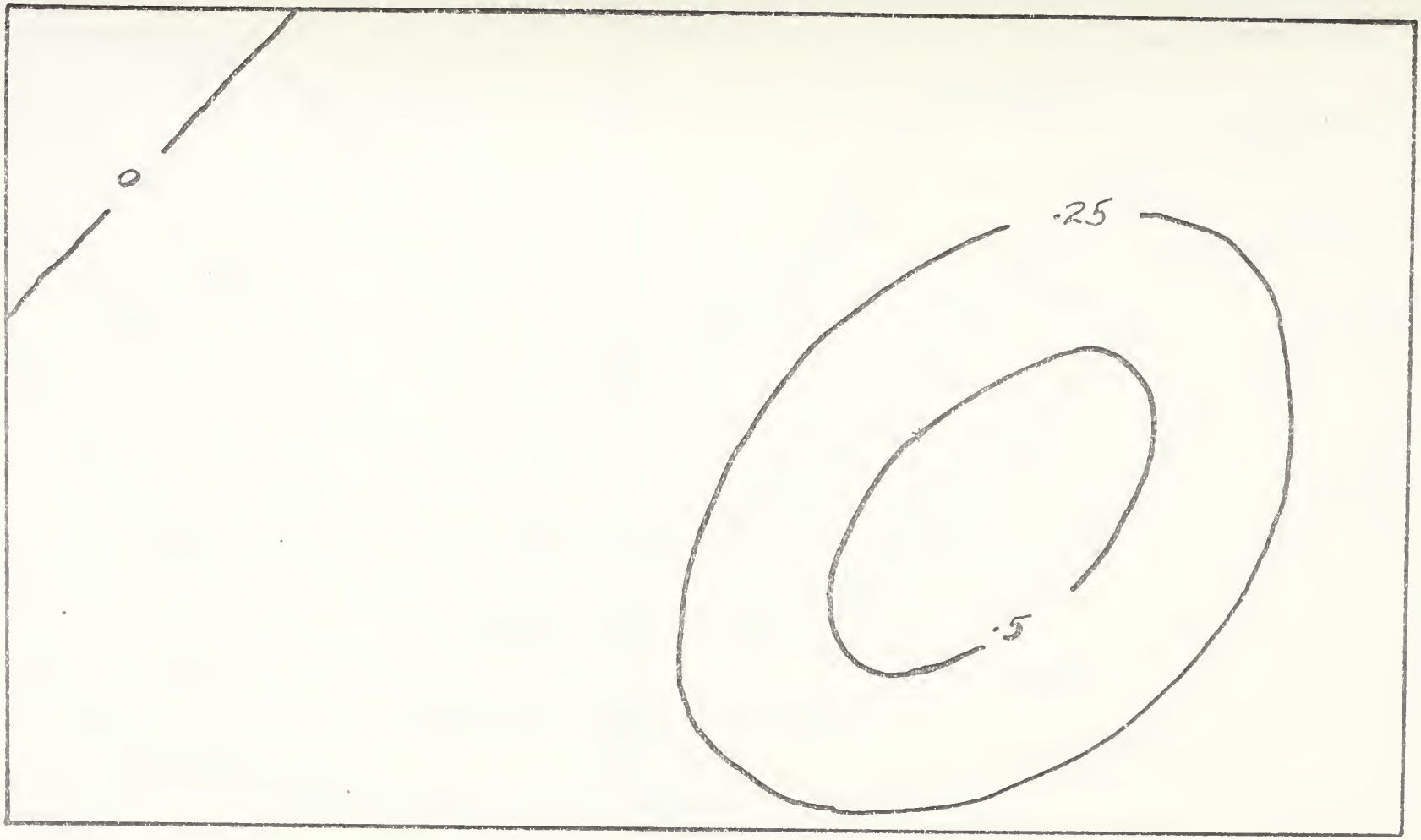

Figure 16. Case III 900 mb condensational heating produced tendency. Units: mb hr^{-1} (+ indicates position of 900 mb low center)

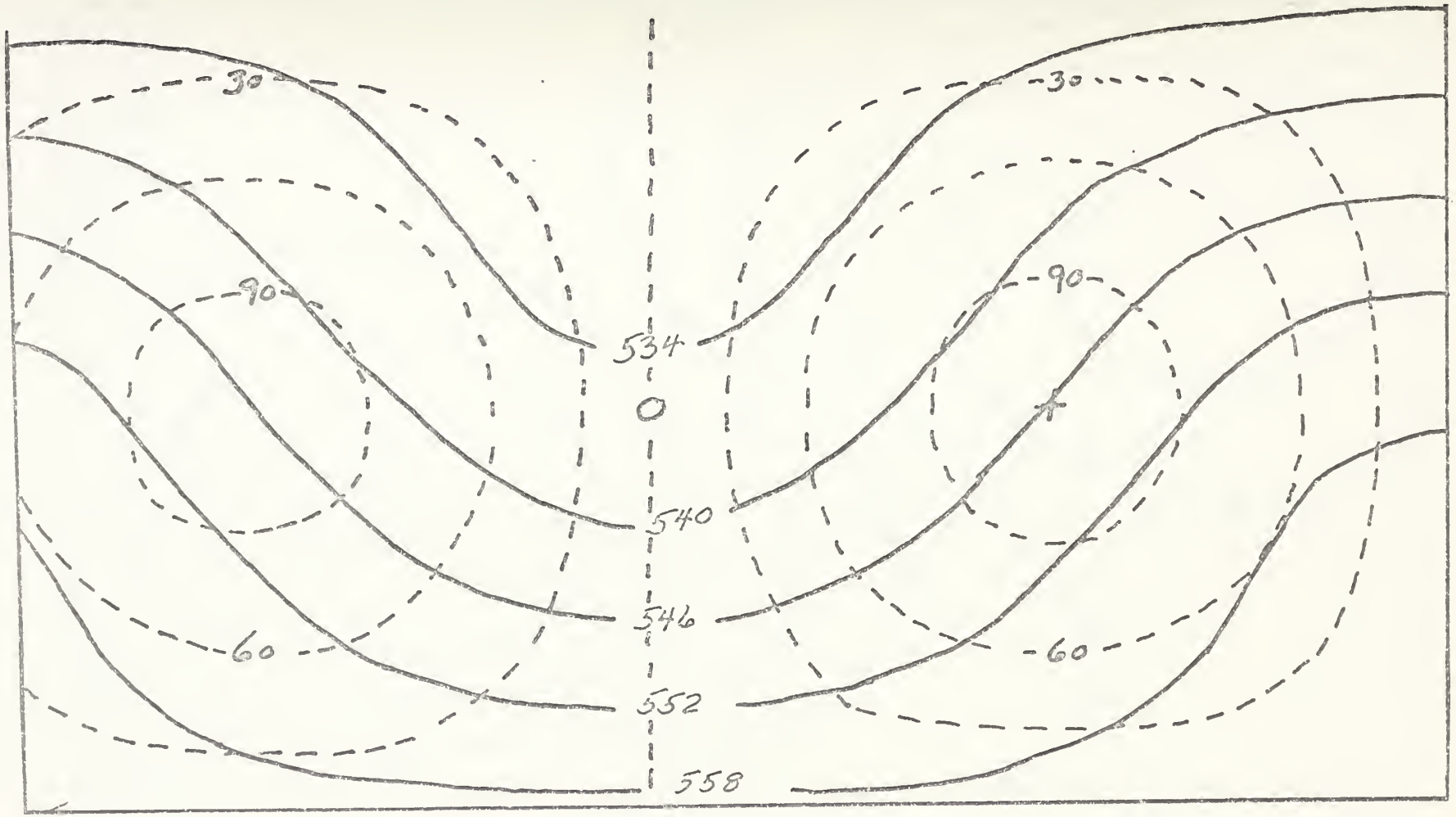

Figure 17. 1000-500 mb thickness (solid line, Units: dm) and 1000 mb contour (dashed lines, Units: m) patterns for analytic model.

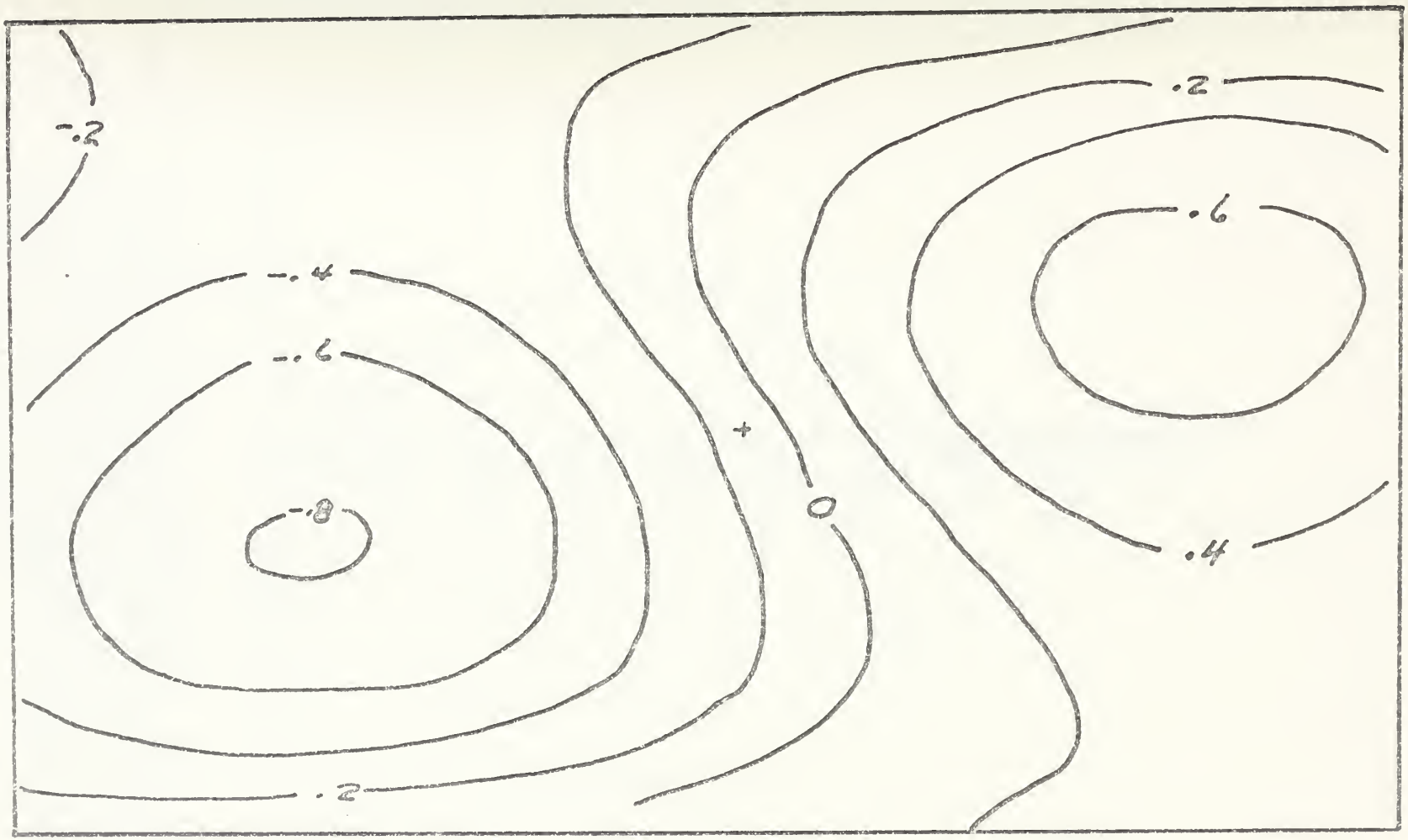

Figure 18. 500 mb thermal advection produced height tendency, divergence effect only.
Units: $10^{-2}m^2sec^{-2}$. (+ indicates 1000 mb low position)

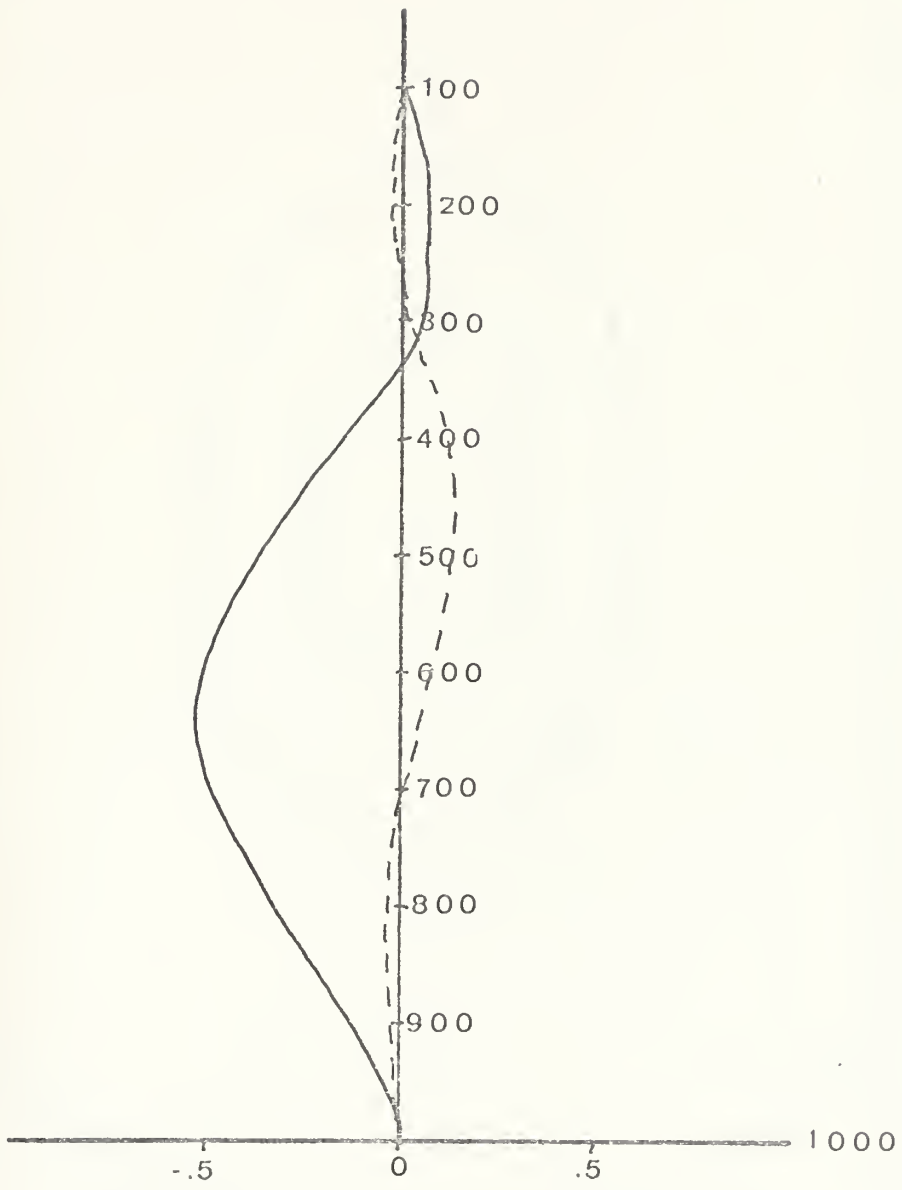

Figure 19. Vertical profile of time rate of change of vertical motion, $\frac{\delta\omega}{\delta t}$, over low center produced by thermal advection (solid line) and by diabatic heating of Case III (dashed line). Units: 10^{-8} cb sec^{-2}

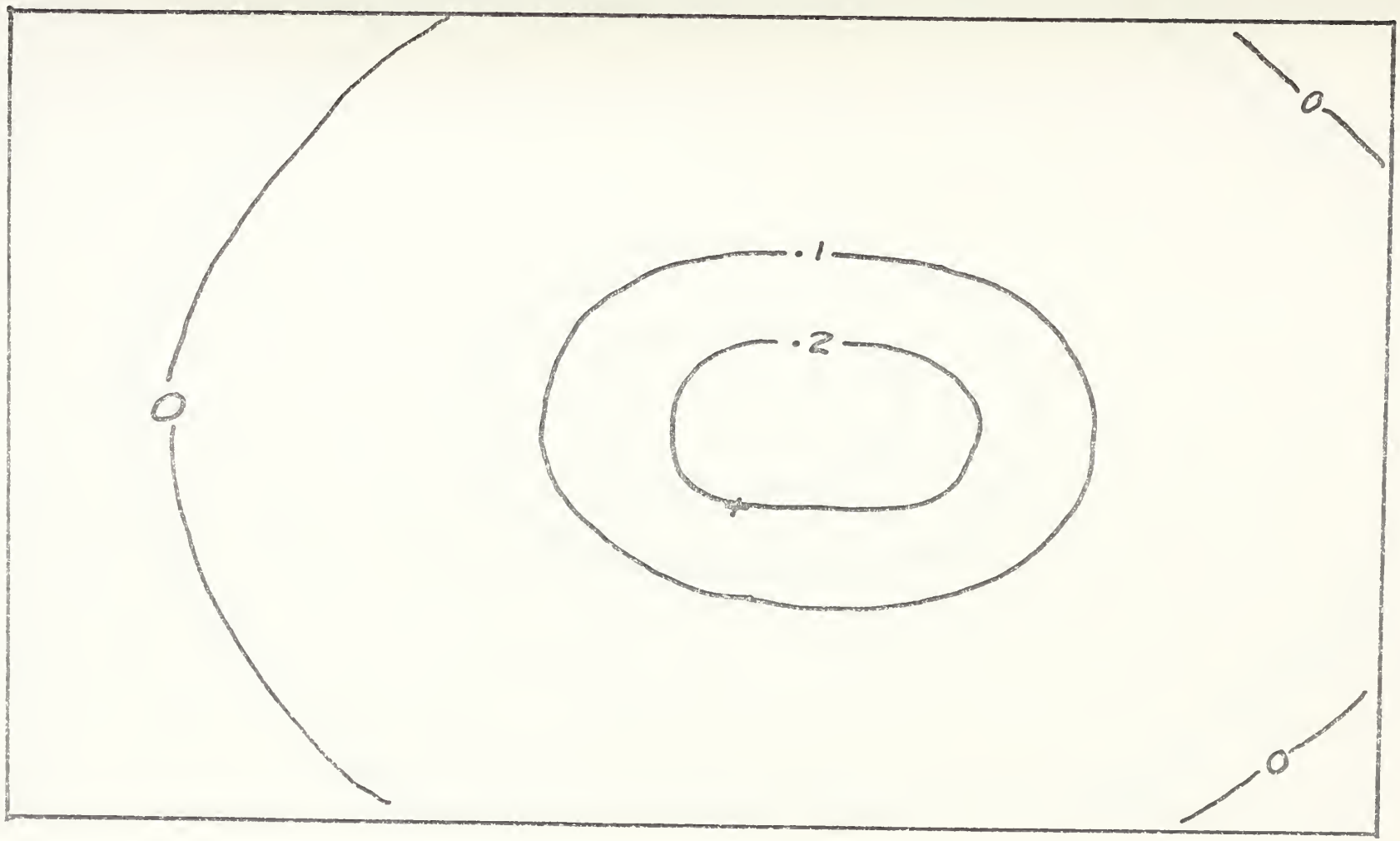

Figure 20. 500 mb condensational heating produced height tendency, divergence effect only for Case I.
Units: $10^{-1}m^2sec^{-2}$
(+ indicates position of 900 mb low center.

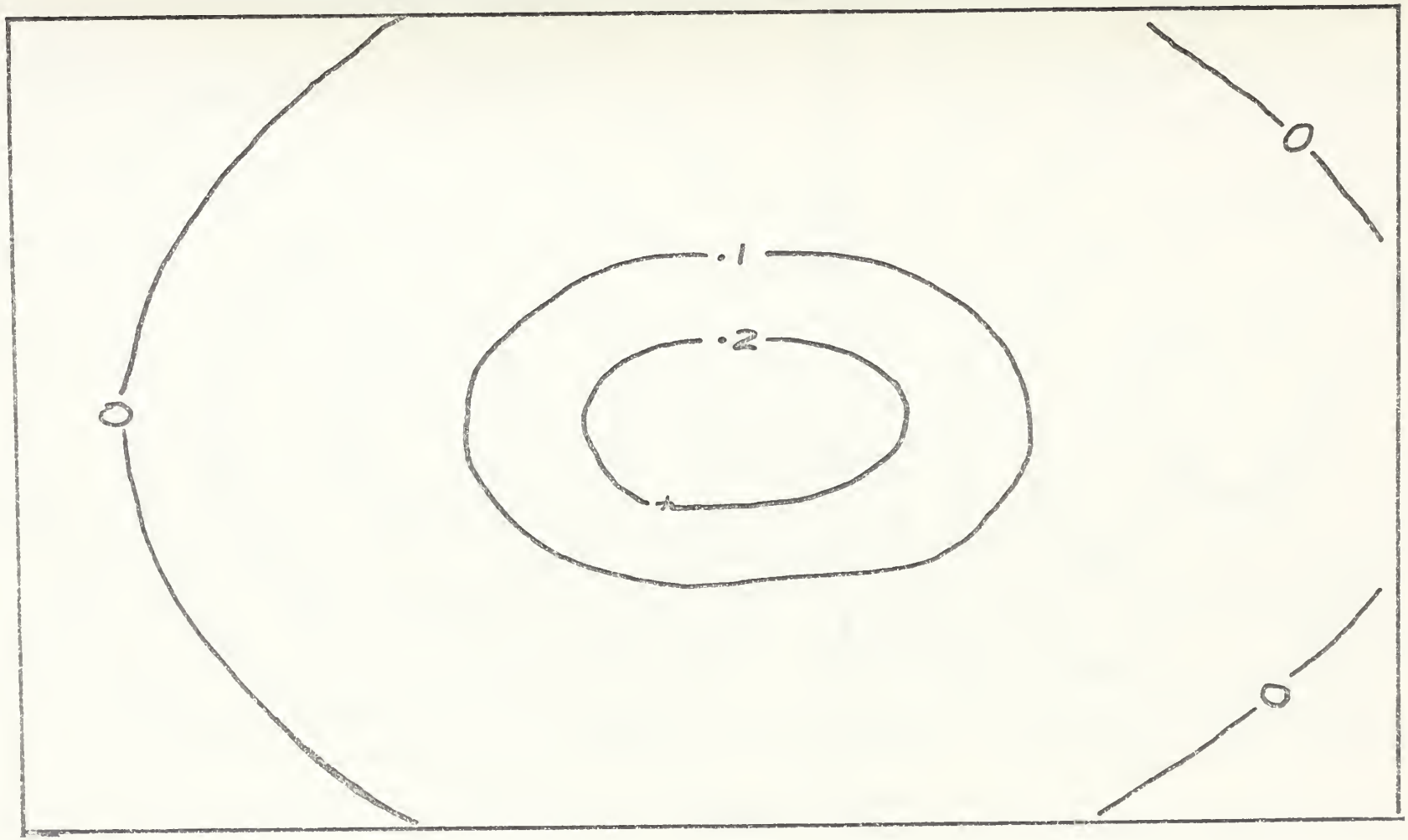

Figure 21. 500 mb condensational heating produced height tendency, divergence effect only, for Case IV.
Units: $10^{-1}m^2sec^{-2}$
(+ indicates 900 mb low center)

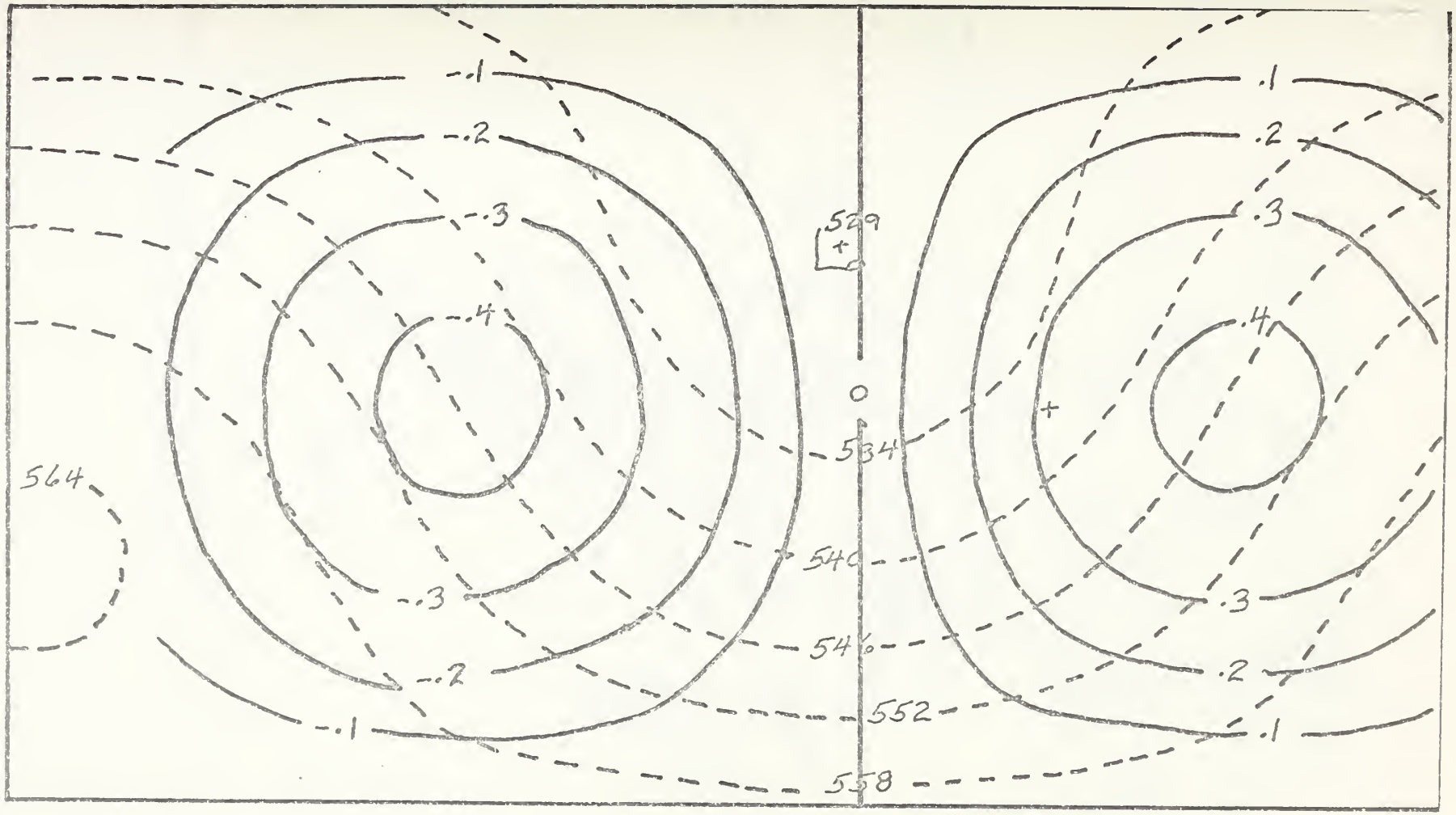

Figure 22. Advection of absolute vorticity for the analytic 500 mb height field.
Units: $10^{-8}sec^{-2}$
(+ indicates 1000 mb low center)

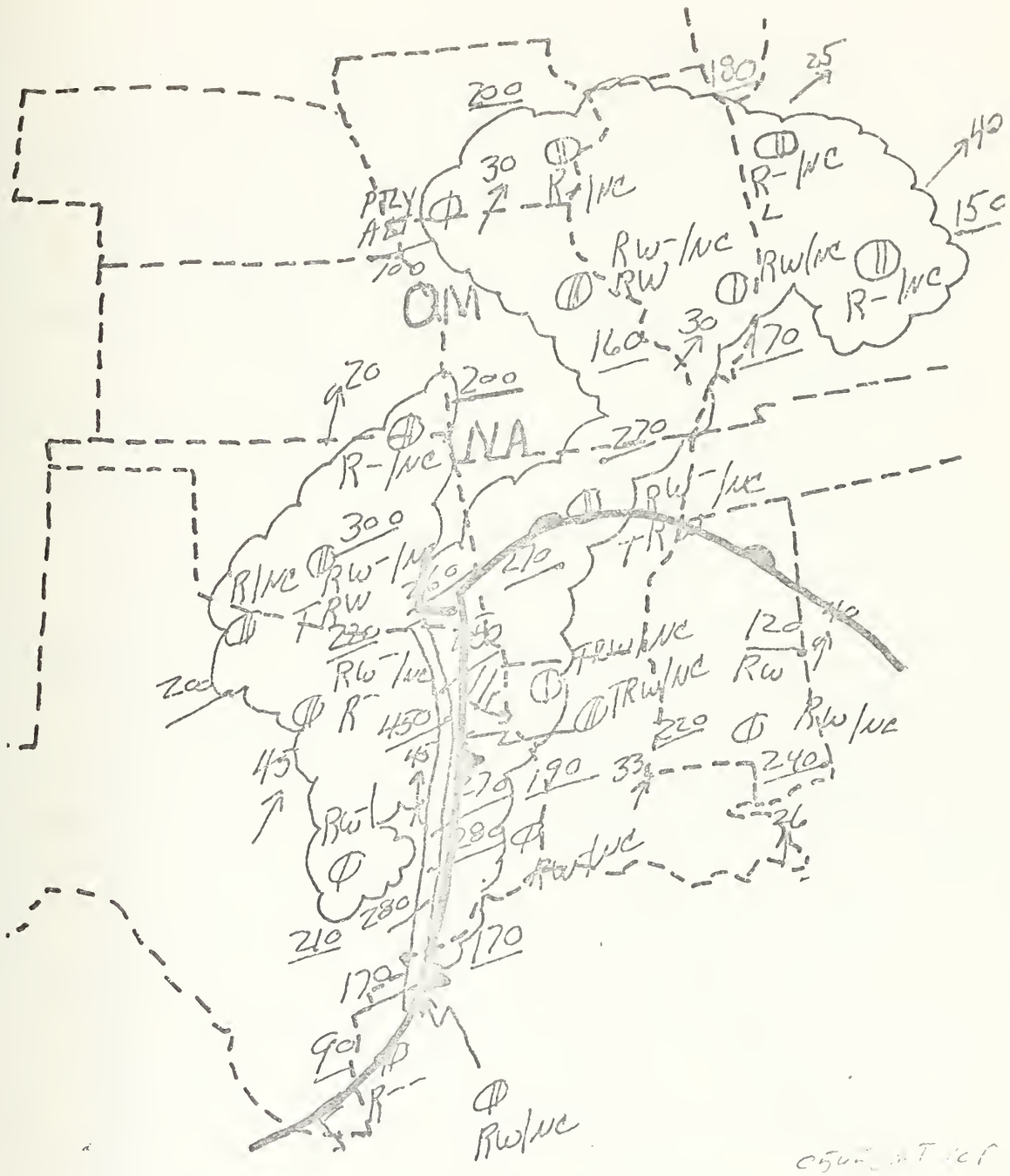

Figure 23. Composite surface-radar summary chart for 0545 GMT 10 December 1971.

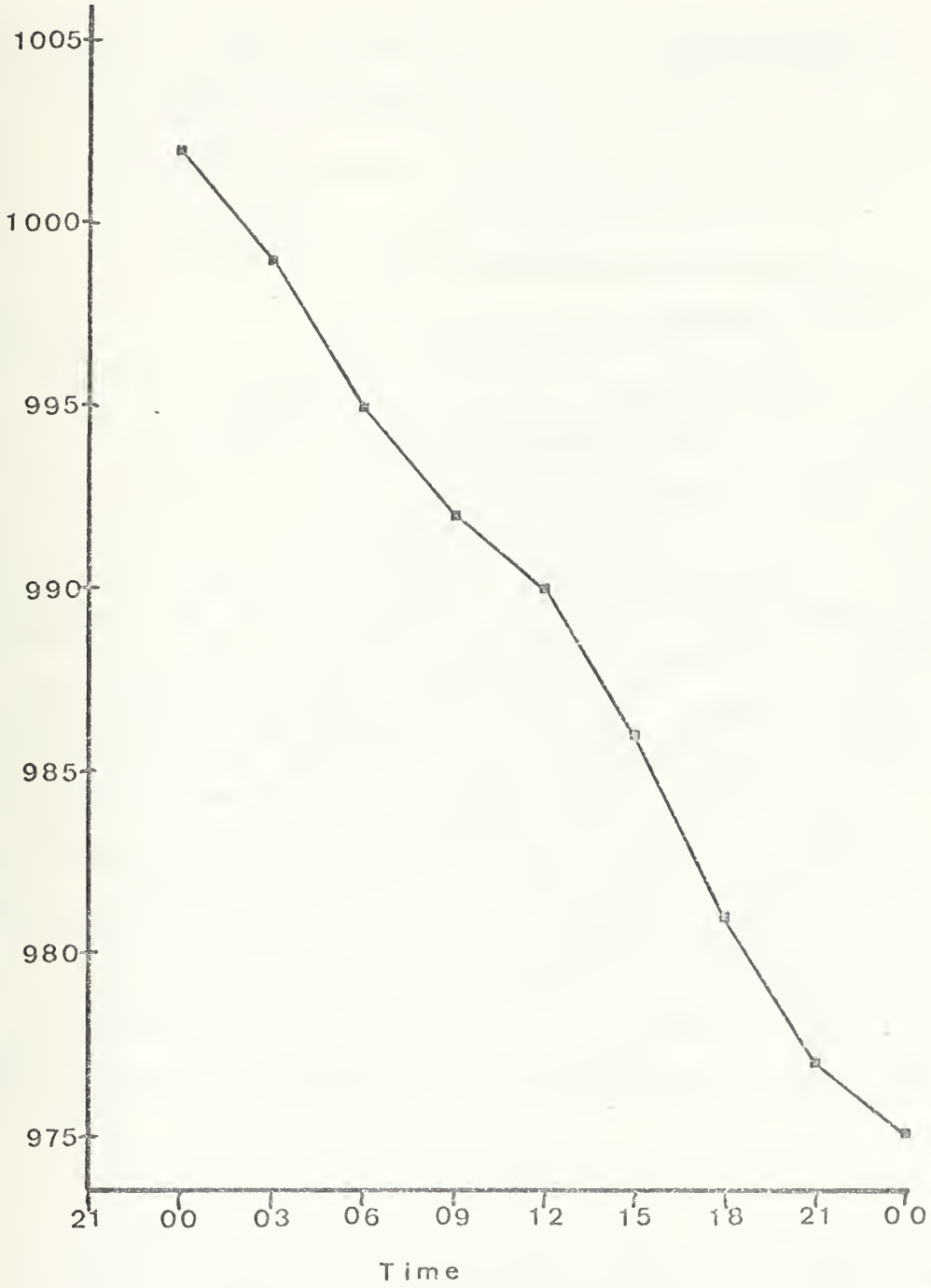

Figure 24. Plot of Central Pressure (Units: mb) versus time (Units: hrs) from 0000 GMT 10 December to 0000 GMT 11 December, 1971

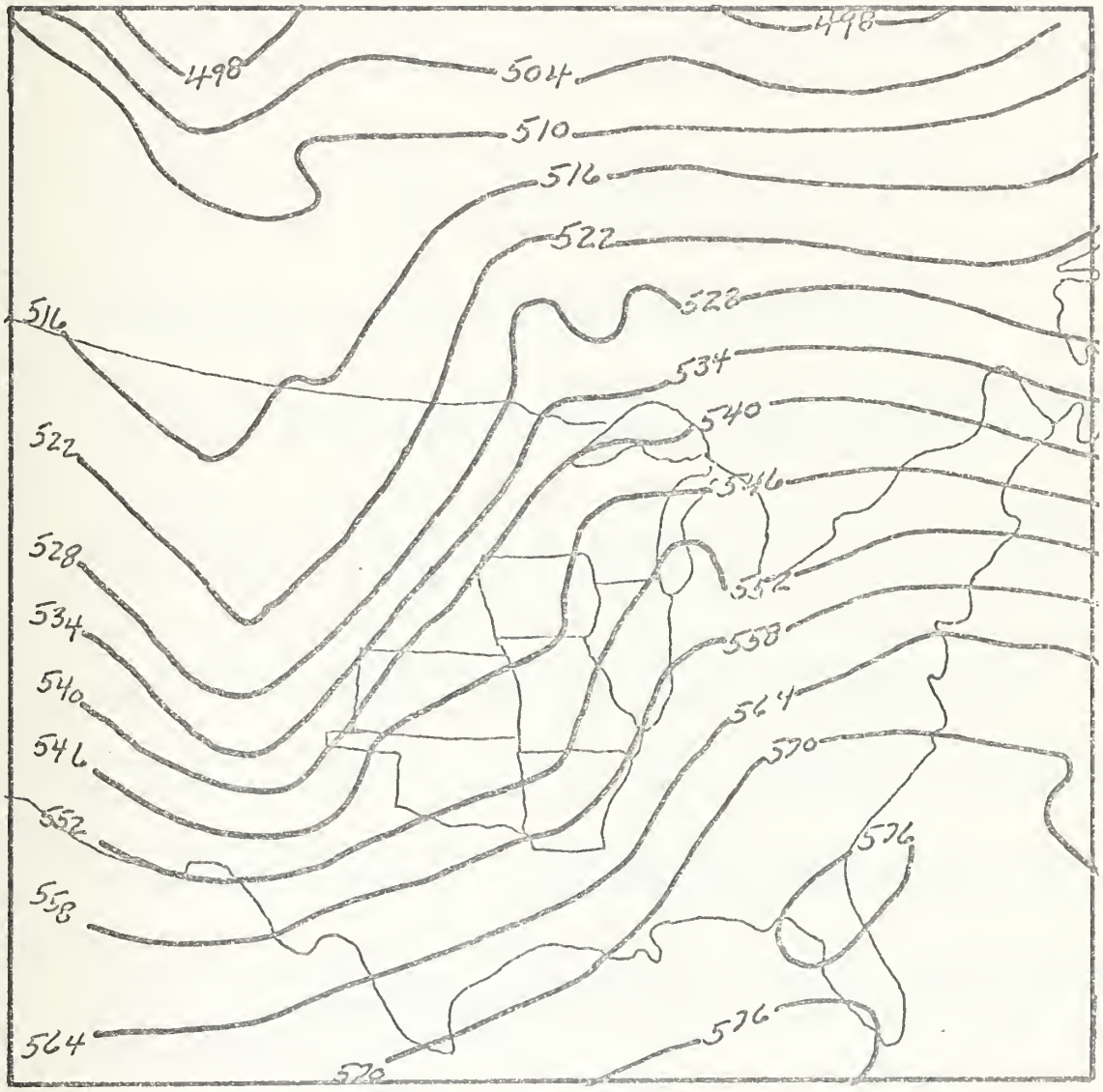

Figure 25. 1000-500 mb thickness pattern for 1200 GMT 10 December 1971. Units: dm (+ indicates 1000 mb low center)

BIBLIOGRAPHY

1. Cressman, G.P., 1959: "An Operational Objective Analysis System," Mon. Wea. Rev., 87, pp. 367-374.

2. Danard, M.B., 1964: On the influence of released latent heat on cyclone development. J. Appl. Meteor., 3, 27-37.

3. Downey, W.K., 1972: The dynamics of the extratropical cyclone - an angular momentum approach. Ph.D. Thesis, Dept. of Met., University of Wisconsin, pp. 264.

4. Holton, J.R., 1972: An Introduction to Dynamic Meteorology. Academic Press, New York, 319 pp.

5. Inman, R.L., 1970: Operational Objective Analysis Schemes at the National Severe Storms Forecast Center, Technical Circular No. 10 National Severe Storms Laboratory.

6. Kasahara, A. and T. Asai, 1967: Effects of an ensemble of convective elements on large-scale motions of the atmosphere. J. Met. Soc. Japan, Ser. 2, 45, pp. 280-290.

7. Kuo, H.L., 1965: On the formation and intensification of tropical cyclones through latent heat release by cumulus convection. J. Atmos. Sci., 22, pp. 40-63.

8. Palmen, E. and C.W. Newton, 1969: Atmospheric Circulation Systems, Academic Press, New York, 603 pp.

9. Petterssen, S., 1956: Weather Analysis and Forecasting. McGraw-Hill Book Co., Inc., New York, 428 pp.

10. Sanders, F., 1971: Analytic solutions of the nonlinear omega and vorticity equations for a structurally simple model of disturbances in the baroclinic Westerlies. Mon. Wea. Rev., 99, pp. 393-407.

11. Stuart, D.W., 1971: Specifications of meso-scale weather from large-scale dynamical calculations. Tech. Rept. No. 70-5, Florida State University, 79 pp.

12. Stuart, D.W., 1974: A comparison of quasi-geostrophic vertical motion using various analyses. Mon. Wea. Rev. 102, pp. 363-374.

13. Sutcliffe, R.C., and A.G. Forsdyke, 1950: The theory and use of upper air thickness patterns in forecasting. Quart. J. Roy. Meteor. Soc., 76, pp. 189-217.

14. Tracton, M.S., 1968: The role of cellular convection with an extratropical cyclone. Proc. Thirteenth Radar Meteor. Conf., Montreal, 216-221.

15. Tracton, M.S., 1973: The role of cumulus convection in the development of extratropical cyclones. Mon. Wea. Rev., 101, 537-592.

INITIAL DISTRIBUTION LIST

		No. Copies
1.	Defense Documentation Center Cameron Station Alexandria, Virginia 22314	2
2.	Library, Code 0212 Naval Postgraduate School Monterey, California 93940	2
3.	Professor M.S. Tracton National Meteorological Center (w 322) Data Assimilation Branch National Weather Service World Weather Building Washington, D.C. 20233	8
4.	Lt. Cecil J. Folker NAVWEASERFAC NAS Pensacola, Florida 32508	2
5.	Meteorology Department, Code 51 Library Naval Postgraduate School Monterey, California 93940	1
6.	Naval Oceanographic Office Library (Code 3330) Washington, D.C. 20373	1
7.	Commander Naval Weather Service Command Naval Weather Service Headquarters Washington Navy Yard Washington, D.C. 20374	1
8.	Fleet Numerical Weather Central Naval Postgraduate School Monterey, California 93940	1
9.	Professor R.T. Williams, Code 51Wu Department of Meteorology Naval Postgraduate School Monterey, California 93940	1

10.	CDR. F.R. Williams, Code 51Wf Department of Meteorology Naval Postgraduate School Monterey, California 93940	1
11.	Professor R.L. Elsberry, Code 51 Es Department of Meteorology Naval Postgraduate School Monterey, California 93940	1

160562

Thesis
F554
c.1

Folker
Quantitative evaluation of the "self-development" process in extratropical cyclogenesis.